Calcolo (2016) 53:487–520
DOI 10.1007/s10092-015-0159-7

Scattering data computation for the Zakharov-Shabat system

L. Fermo[1] · **C. van der Mee**[1] · **S. Seatzu**[1]

Received: 16 February 2015 / Accepted: 8 October 2015 / Published online: 16 November 2015

Abstract A numerical method to compute the scattering data for the Zakharov-Shabat system associated to the initial value problem for the nonlinear Schrödinger equation is proposed. The method involves the numerical solution of Volterra integral systems with structured kernels, of structured integral equations in unbounded domains and the identification of coefficients and parameters appearing in monomial-exponential sums. Numerical experiments confirm the effectiveness of the proposed technique.

Keywords Nonlinear Schrödinger equation · Inverse scattering transform · Integral equations

Mathematics Subject Classification 41A46 · 65R20 · 35P25

1 Introduction

The problem we are addressing concerns the numerical computation of the scattering data of the Zakharov-Shabat (ZS) system associated to the initial value problem (IVP) for the nonlinear Schrödinger (NLS) equation

✉ L. Fermo
fermo@unica.it

C. van der Mee
cornelis@krein.unica.it

S. Seatzu
seatzu@unica.it

[1] Department of Mathematics and Computer Science, University of Cagliari, Viale Merello 92, 09123 Cagliari, Italy

$$\begin{cases} \mathbf{i}u_t + u_{xx} \pm 2|u|^2 u = 0, \quad x \in \mathbb{R}, \quad t > 0 \\ u(x,0) = u_0(x), \quad x \in \mathbb{R} \end{cases} \tag{1}$$

where $\mathbf{i}$ denotes the imaginary unit, $u = u(x,t)$ is the unknown potential, the subscripts x and t designate partial derivatives with respect to position and time, $u_0 \in L^1(\mathbb{R})$ is the initial potential and the $\pm$ sign depends on symmetry properties of u. The plus sign regards the focusing case and the minus sign the defocusing case.

This equation has important physical applications, as it arises in modeling signal processing in optical fibers [12], as well as in surface waves on deep water [1,2].

As Zakharov and Shabat proved [17], Eq. (1) can be associated to the first order system of ordinary differential equations

$$\mathbf{i}\mathbf{J}\frac{\partial \mathbf{\Psi}}{\partial x}(\lambda, x) - \mathbf{V}(x)\mathbf{\Psi}(\lambda, x) = \lambda \mathbf{\Psi}(\lambda, x), \quad x \in \mathbb{R} \tag{2}$$

where $\lambda \in \mathbb{C}$ is a spectral parameter and

$$\mathbf{J} = \begin{pmatrix} 1 & 0 \\ 0 & -1 \end{pmatrix}, \qquad \mathbf{V} = \mathbf{i}\begin{pmatrix} 0 & u_0 \\ v_0 & 0 \end{pmatrix} \tag{3}$$

with $v_0 = u_0^*$ in the focusing case and $v_0 = -u_0^*$ in the defocusing case. Here and in the sequel the asterisk denotes the complex conjugate.

With the help of this system, known as the ZS system, the solution of the IVP of (1) can theoretically be obtained from the initial potential u_0 by means of the so-called Inverse Scattering Transform (IST) technique. In fact, it can be obtained by performing the following three steps:

(a) starting from the initial potential u_0, solve the ZS system associated to the NLS to obtain the initial scattering data;
(b) propagate the initial scattering data in time;
(c) solve the corresponding inverse scattering problem for the ZS system, i.e. determine the solution of (1) from the scattering data evolved in time.

While an effective numerical method to solve steps (b) and (c) exists [4], to the best of our knowledge an effective method to compute all the scattering data for the ZS system does not exist.

The method proposed by Osborne [11], Wahls and Poor [18], in particular, as well as that one proposed by Trogdon and Olver [14,15] are aimed at approximating only some of the scattering data, specifically the reflection and transmission coefficients. Hence, none of these allows one to compute all the initial scattering data needed to solve steps (b) and (c), which is the aim of this paper. As a result, our method should be the only numerical method suitable to compute all the scattering data for the ZS system and then to solve the NLS by means of the numerical method proposed in [4].

The paper is organized as follows. In Sect. 2 we recall the definition of the scattering data, as well as the properties necessary for the illustration of the various steps of our method. Section 3 is devoted to the definition and properties of auxiliary functions which are basic, in our method, to the characterization of the scattering data. In Sect.

4 we illustrate the steps we have to take, once the auxiliary functions have been computed. The algorithms of the method we propose to compute all the scattering data for the ZS system are illustrated in Sect. 5. In Sect. 6 we introduce two different potentials for which the numerical results are given in Sect. 7. Finally, we conclude the paper by an Appendix concerning the study of the support of the auxiliary functions introduced in Sect. 3.

2 Definition and properties

To recall the definitions and the most important properties of this paper, we start with that of Jost solutions [3], that is with the solution of the ZS system which satisfy the asymptotic conditions

$$(\bar{\boldsymbol{\Psi}}(\lambda, x),\ \boldsymbol{\Psi}(\lambda, x)) = e^{-\mathrm{i}\lambda \mathbf{J} x}(\mathbf{I} + o(1)), \quad x \to +\infty \tag{4}$$

$$(\boldsymbol{\Phi}(\lambda, x),\ \bar{\boldsymbol{\Phi}}(\lambda, x)) = e^{-\mathrm{i}\lambda \mathbf{J} x}(\mathbf{I} + o(1)), \quad x \to -\infty \tag{5}$$

where $\lambda \in \mathbb{R}$, $\mathbf{I}$ denotes the identity matrix and $\mathbf{J}$ is defined in (3).

Since these solutions satisfy the same linear first order system, there exist transition matrices

$$\mathbf{A}_\ell(\lambda) = \begin{pmatrix} a_{\ell 1}(\lambda) & a_{\ell 2}(\lambda) \\ a_{\ell 3}(\lambda) & a_{\ell 4}(\lambda) \end{pmatrix}, \qquad \mathbf{A}_r(\lambda) = \mathbf{A}_\ell(\lambda)^{-1} = \begin{pmatrix} a_{r1}(\lambda) & a_{r2}(\lambda) \\ a_{r3}(\lambda) & a_{r4}(\lambda) \end{pmatrix} \tag{6}$$

such that

$$(\bar{\boldsymbol{\Psi}}(\lambda, x),\ \boldsymbol{\Psi}(\lambda, x)) = (\boldsymbol{\Phi}(\lambda, x),\ \bar{\boldsymbol{\Phi}}(\lambda, x))\mathbf{A}_\ell(\lambda)$$

$$(\boldsymbol{\Phi}(\lambda, x),\ \bar{\boldsymbol{\Phi}}(\lambda, x)) = (\bar{\boldsymbol{\Psi}}(\lambda, x),\ \boldsymbol{\Psi}(\lambda, x))\mathbf{A}_r(\lambda).$$

Denoting by $\mathbb{C}^+$ and $\mathbb{C}^-$ the upper and lower half plane and by $\bar{\mathbb{C}}^+$ and $\bar{\mathbb{C}}^-$ their closures, respectively, the following analytic properties hold true. The Jost functions $\boldsymbol{\Psi}(\lambda, x)$ and $\boldsymbol{\Phi}(\lambda, x)$ are continuous in $\lambda \in \bar{\mathbb{C}}^+$, are analytic in $\lambda \in \mathbb{C}^+$, and have finite limits as $\lambda \to \infty$ in $\bar{\mathbb{C}}^+$, whereas $\bar{\boldsymbol{\Psi}}(\lambda, x)$ and $\bar{\boldsymbol{\Phi}}(\lambda, x)$ are continuous in $\lambda \in \bar{\mathbb{C}}^-$, are analytic in $\lambda \in \mathbb{C}^-$, and have finite limits as $\lambda \to \infty$ in $\bar{\mathbb{C}}^-$. We can then rewrite (4) and (5) as the Riemann-Hilbert problem

$$(\bar{\boldsymbol{\Psi}}(\lambda, x),\ \bar{\boldsymbol{\Phi}}(\lambda, x)) = (\boldsymbol{\Phi}(\lambda, x),\ \boldsymbol{\Psi}(\lambda, x))\,\mathbf{J}\,\mathbf{S}(\lambda)\,\mathbf{J}$$

where

$$\mathbf{S}(\lambda) = \begin{pmatrix} T(\lambda) & L(\lambda) \\ R(\lambda) & T(\lambda) \end{pmatrix}.$$

Here $T(\lambda)$ represents the transmission coefficient, while $L(\lambda)$ and $R(\lambda)$ stand for the reflection coefficients from the left and from the right, respectively. This spectral matrix satisfies the following symmetry properties [16]

$$\mathbf{S}^\dagger(\lambda)\mathbf{S}(\lambda) = \mathbf{S}(\lambda)\mathbf{S}^\dagger(\lambda) = \mathbf{I} \tag{7}$$

in the defocusing case and

$$\mathbf{S}^{\dagger}(\lambda)\,\mathbf{J}\,\mathbf{S}(\lambda) = \mathbf{S}(\lambda)\,\mathbf{J}\,\mathbf{S}^{\dagger}(\lambda) = \mathbf{J} \tag{8}$$

in the focusing case, where $\mathbf{I}$ denotes the identity matrix and $\mathbf{J}$ was introduced in (3). Here and in the sequel the dagger denotes the matrix conjugate transpose. The numerical validity of these properties is used in Sect. 7 to check the effectiveness of our algorithm.

If $T(\lambda)$ has no poles in the complex upper half plane $\mathbb{C}^+$ (as occurs in the defocusing case), the transmission coefficient and the reflection coefficients are the only scattering data to identify. Otherwise, denoting by $\lambda_1, \ldots, \lambda_n$ the so-called bound states, that is the finitely many poles of $T(\lambda)$ in $\mathbb{C}^+$, and by $m_1, \ldots, m_n$ the corresponding multiplicities, we have to identify the parameters $\{n, m_j, \lambda_j\}$ as well as the coefficients $\{(\Gamma_\ell)_{js}, (\Gamma_r)_{js}\}$ of the initial spectral sums from the left and from the right

$$S_\ell(\alpha) = \sum_{j=1}^{n} e^{i\lambda_j \alpha} \sum_{s=0}^{m_j-1} (\Gamma_\ell)_{js} \frac{\alpha^s}{s!}, \quad \alpha \geq 0 \tag{9}$$

$$S_r(\alpha) = \sum_{j=1}^{n} e^{i\lambda_j^* \alpha} \sum_{s=0}^{m_j-1} (\Gamma_r)_{js} \frac{\alpha^s}{s!}, \quad \alpha \leq 0. \tag{10}$$

In (9) and (10) the coefficients $(\Gamma_\ell)_{js}$ and $(\Gamma_r)_{js}$ are the so-called norming constants from the left and from the right, respectively, and $0! = 1$.

Our method allows us to compute all the scattering data, i.e. the spectral matrix as well as the discrete scattering data $\{\lambda_j, (\Gamma_\ell)_{js}, (\Gamma_r)_{js}\}$ whenever they exist.

For the identification of the discrete spectral data, a crucial role is played by the Marchenko kernels from the left $\Omega_\ell(\alpha)$ and from the right $\Omega_r(\alpha)$ whose analytical characterization is postponed to Sect. 4. These two kernels are connected to the above spectral coefficients and spectral sums as follows:

$$\Omega_\ell(\alpha) = \rho(\alpha) + S_\ell(\alpha), \quad \text{for} \quad \alpha \geq 0 \tag{11}$$

$$\Omega_r(\alpha) = \ell(\alpha) + S_r(\alpha), \quad \text{for} \quad \alpha \leq 0 \tag{12}$$

where

$$\rho(\alpha) = \frac{1}{2\pi} \int_{-\infty}^{+\infty} R(\lambda) e^{i\lambda\alpha} d\lambda = \mathcal{F}^{-1}\{R(\lambda)\} \tag{13}$$

is the inverse Fourier transform of the reflection coefficient from the right $R(\lambda)$ and

$$\ell(\alpha) = \frac{1}{2\pi} \int_{-\infty}^{+\infty} L(\lambda) e^{-i\lambda\alpha} d\lambda = \frac{1}{2\pi} \mathcal{F}\{L(\lambda)\}, \tag{14}$$

apart from the factor $1/2\pi$, is the Fourier transform of the reflection coefficient from the left $L(\lambda)$.

We note that $\Omega_\ell(\alpha)$ and $\Omega_r(\alpha)$, respectively, reduce to:

(a) $S_\ell(\alpha)$ and $S_r(\alpha)$ if the reflection coefficients vanish (reflectionless case). This situation occurs for initial potentials leading to N-soliton NLS solutions.
(b) $\rho(\alpha)$ and $\ell(\alpha)$ if there are no bound states. This situation occurs in the defocusing case and whenever $\|u_0\|_1 = \|v_0\|_1 < \frac{\pi}{2}$ [10].

3 Auxiliary functions

In this section we introduce four pairs of auxiliary functions and the Volterra integral equations that characterize them. Their solution, as shown in the next section (see also [7,16]), is fundamental for computing the initial Marchenko kernels as well as $\rho(\alpha)$ and $\ell(\alpha)$.

Following [7], let us introduce, for $y \geq x$, the two pairs of unknown auxiliary functions

$$\bar{\mathbf{K}}(x,y) \equiv \begin{pmatrix} \bar{K}^{\,\mathrm{up}}(x,y) \\ \bar{K}^{\,\mathrm{dn}}(x,y) \end{pmatrix}, \quad \mathbf{K}(x,y) \equiv \begin{pmatrix} K^{\,\mathrm{up}}(x,y) \\ K^{\,\mathrm{dn}}(x,y) \end{pmatrix},$$

and, for $y \leq x$, the two pairs of unknown auxiliary functions

$$\bar{\mathbf{M}}(x,y) \equiv \begin{pmatrix} \bar{M}^{\,\mathrm{up}}(x,y) \\ \bar{M}^{\,\mathrm{dn}}(x,y) \end{pmatrix}, \quad \mathbf{M}(x,y) \equiv \begin{pmatrix} M^{\,\mathrm{up}}(x,y) \\ M^{\,\mathrm{dn}}(x,y) \end{pmatrix}.$$

For the sake of clarity, let us explain how these functions are connected to the Jost matrices associated to the ZS system (2).

As in [3,16], we represent the 2×2 Jost matrices as the Fourier transforms of the pairs of auxiliary functions:

$$(\bar{\boldsymbol{\Psi}}(\lambda,x), \boldsymbol{\Psi}(\lambda,x)) = e^{-i\lambda \mathbf{J} x} + \int_x^\infty \left(\bar{\mathbf{K}}(x,y), \mathbf{K}(x,y)\right) e^{-i\lambda \mathbf{J} y}\, dy, \tag{15}$$

$$(\boldsymbol{\Phi}(\lambda,x), \bar{\boldsymbol{\Phi}}(\lambda,x)) = e^{-i\lambda \mathbf{J} x} + \int_{-\infty}^x \left(\mathbf{M}(x,y), \bar{\mathbf{M}}(x,y)\right) e^{-i\lambda \mathbf{J} y}\, dy, \tag{16}$$

from which inverting the Fourier transforms we get

$$(\bar{\mathbf{K}}(x,y), \mathbf{K}(x,y)) = \frac{1}{2\pi} \int_{-\infty}^\infty \left[(\bar{\boldsymbol{\Psi}}(\lambda,x), \boldsymbol{\Psi}(\lambda,x)) - e^{-i\lambda \mathbf{J} x} \right] e^{i\lambda \mathbf{J} y}\, d\lambda, \tag{17}$$

$$(\mathbf{M}(x,y), \bar{\mathbf{M}}(x,y)) = \frac{1}{2\pi} \int_{-\infty}^\infty \left[(\boldsymbol{\Phi}(\lambda,x), \bar{\boldsymbol{\Phi}}(\lambda,x)) - e^{-i\lambda \mathbf{J} x} \right] e^{i\lambda \mathbf{J} y}\, d\lambda. \tag{18}$$

Now, for $y \geq x$, the pair $(\bar{K}^{\,\mathrm{up}}, \bar{K}^{\,\mathrm{dn}})$ is the solution of the following system of two structured Volterra integral equations [7,16]:

$$\begin{cases} \bar{K}^{\,\mathrm{up}}(x,y) + \displaystyle\int_x^{\infty} u_0(z)\,\bar{K}^{\,\mathrm{dn}}(z, z+y-x)\,dz = 0 \\ \\ \bar{K}^{\,\mathrm{dn}}(x,y) - \displaystyle\int_x^{\frac{1}{2}(x+y)} v_0(z)\,\bar{K}^{\,\mathrm{up}}(z, x+y-z)\,dz = \tfrac{1}{2} v_0\left(\tfrac{1}{2}(x+y)\right) \end{cases} \tag{19}$$

while the pair $(K^{\,\mathrm{up}},\ K^{\,\mathrm{dn}})$ is the solution of the system

$$\begin{cases} K^{\,\mathrm{up}}(x,y) + \displaystyle\int_x^{\frac{1}{2}(x+y)} u_0(z)\,K^{\,\mathrm{dn}}(z, x+y-z)\,dz = -\tfrac{1}{2} u_0\left(\tfrac{1}{2}(x+y)\right) \\ \\ K^{\,\mathrm{dn}}(x,y) - \displaystyle\int_x^{\infty} v_0(z)\,K^{\,\mathrm{up}}(z, z+y-x)\,dz = 0. \end{cases} \tag{20}$$

Similarly, for $y \le x$ the pair $(\bar{M}^{\,\mathrm{up}},\ \bar{M}^{\,\mathrm{dn}})$ is the solution of the system of two structured Volterra equations:

$$\begin{cases} \bar{M}^{\,\mathrm{up}}(x,y) - \displaystyle\int_{\frac{1}{2}(x+y)}^{x} u_0(z)\,\bar{M}^{\,\mathrm{dn}}(z, x+y-z)\,dz = \tfrac{1}{2} u_0\left(\tfrac{1}{2}(x+y)\right) \\ \\ \bar{M}^{\,\mathrm{dn}}(x,y) + \displaystyle\int_{-\infty}^{x} v_0(z)\,\bar{M}^{\,\mathrm{up}}(z, z+y-x)\,dz = 0 \end{cases} \tag{21}$$

and the pair $(M^{\,\mathrm{up}},\ M^{\,\mathrm{dn}})$ is the solution of the following system

$$\begin{cases} M^{\,\mathrm{up}}(x,y) - \displaystyle\int_{-\infty}^{x} u_0(z)\,M^{\,\mathrm{dn}}(z, z+y-x)\,dz = 0 \\ \\ M^{\,\mathrm{dn}}(x,y) + \displaystyle\int_{\frac{1}{2}(x+y)}^{x} v_0(z)\,M^{\,\mathrm{up}}(z, x+y-z)\,dz = -\tfrac{1}{2} v_0(\tfrac{1}{2}(x+y)). \end{cases} \tag{22}$$

From the computational point of view, on the bisector $y = x$, it is important to note that each auxiliary function is uniquely determined by the initial solution or its partial integral energy. In fact, setting $y = x$ in each of the four Volterra systems, we immediately obtain:

$$\bar{K}^{\,\mathrm{dn}}(x,x) = \frac{1}{2} v_0(x), \quad \bar{K}^{\,\mathrm{up}}(x,x) = -\frac{1}{2}\int_x^{\infty} u_0(z)\,v_0(z)\,dz, \tag{23}$$

$$K^{\,\mathrm{up}}(x,x) = -\frac{1}{2} u_0(x), \quad K^{\,\mathrm{dn}}(x,x) = -\frac{1}{2}\int_x^{\infty} u_0(z)\,v_0(z)\,dz, \tag{24}$$

$$M^{\,\mathrm{dn}}(x,x) = -\frac{1}{2} v_0(x), \quad M^{\,\mathrm{up}}(x,x) = -\frac{1}{2}\int_{-\infty}^{x} u_0(z)\,v_0(z)\,dz, \tag{25}$$

$$\bar{M}^{\,\mathrm{up}}(x,x) = \frac{1}{2} u_0(x), \quad \bar{M}^{\,\mathrm{dn}}(x,x) = -\frac{1}{2}\int_{-\infty}^{x} u_0(z)\,v_0(z)\,dz. \tag{26}$$

Moreover, let us mention that the vector functions $\bar{\mathbf{K}}$ and $\mathbf{K}$, as well as the functions $\bar{\mathbf{M}}$ and $\mathbf{M}$, are related to each other. Indeed, in the focusing case the following symmetry properties hold true [16]:

$$\begin{pmatrix} K^{\,\mathrm{up}}(x,y) \\ K^{\,\mathrm{dn}}(x,y) \end{pmatrix} = \begin{pmatrix} -\bar{K}^{\,\mathrm{dn}}(x,y)^* \\ \bar{K}^{\,\mathrm{up}}(x,y)^* \end{pmatrix}, \qquad \begin{pmatrix} M^{\,\mathrm{up}}(x,y) \\ M^{\,\mathrm{dn}}(x,y) \end{pmatrix} = \begin{pmatrix} \bar{M}^{\,\mathrm{dn}}(x,y)^* \\ -\bar{M}^{\,\mathrm{up}}(x,y)^* \end{pmatrix} \tag{27}$$

while in the defocusing case the following symmetry relations can be proved:

$$\begin{pmatrix} K^{\,\mathrm{up}}(x,y) \\ K^{\,\mathrm{dn}}(x,y) \end{pmatrix} = \begin{pmatrix} \bar{K}^{\,\mathrm{dn}}(x,y)^* \\ \bar{K}^{\,\mathrm{up}}(x,y)^* \end{pmatrix}, \qquad \begin{pmatrix} M^{\,\mathrm{up}}(x,y) \\ M^{\,\mathrm{dn}}(x,y) \end{pmatrix} = \begin{pmatrix} \bar{M}^{\,\mathrm{dn}}(x,y)^* \\ \bar{M}^{\,\mathrm{up}}(x,y)^* \end{pmatrix}. \tag{28}$$

Remark 1 Let us note that, in virtue of (27), (28), we only need to solve numerically systems (19) and (21) or systems (20) and (22) and then compute the remaining auxiliary functions by resorting to the above symmetry properties .

Remark 2 If the potentials u_0 and v_0 are even functions, the auxiliary functions $\mathbf{M}$ and $\mathbf{M}$ can easily be obtained from the functions $\bar{\mathbf{K}}$ and $\mathbf{K}$ as follows:

$$\begin{aligned} M^{\,\mathrm{up}}(x,y) &= \bar{K}^{\,\mathrm{up}}(-x,-y) \qquad & M^{\,\mathrm{dn}}(x,y) &= -\bar{K}^{\,\mathrm{dn}}(-x,-y) \\ \bar{M}^{\,\mathrm{up}}(x,y) &= -K^{\,\mathrm{up}}(-x,-y) \qquad & \bar{M}^{\,\mathrm{dn}}(x,y) &= K^{\,\mathrm{dn}}(-x,-y). \end{aligned}$$

Similarly, if the potentials u_0 and v_0 are odd functions, we have

$$\begin{aligned} M^{\,\mathrm{up}}(x,y) &= \bar{K}^{\,\mathrm{up}}(-x,-y) \qquad & M^{\,\mathrm{dn}}(x,y) &= \bar{K}^{\,\mathrm{dn}}(-x,-y) \\ \bar{M}^{\,\mathrm{up}}(x,y) &= K^{\,\mathrm{up}}(-x,-y) \qquad & \bar{M}^{\,\mathrm{dn}}(x,y) &= K^{\,\mathrm{dn}}(-x,-y). \end{aligned}$$

Consequently, in these cases we only need to solve numerically one system, for instance system (19).

4 Initial Marchenko kernels, scattering matrix and Fourier transforms of reflection coefficients

This section consists of two parts. In the first part we recall the Volterra integral equations that we solve to obtain the initial Marchenko kernels $\Omega_\ell(\alpha)$ and $\Omega_r(\alpha)$. In the second part we explain how to compute the scattering matrix and the Fourier transforms of the reflection coefficients R and L.

4.1 Initial Marchenko kernels

Following [16, 2.50a and 2.50b] we can say that, for $y \geq x \geq 0$, the Marchenko kernel Ω_ℓ is connected to the auxiliary functions $K^{\,\mathrm{dn}}$ and $\bar{K}^{\,\mathrm{dn}}$ as follows:

$$\Omega_\ell(x+y) + \int_x^\infty K^{\,\mathrm{dn}}(x,z)\,\Omega_\ell(z+y)\,dz = -\bar{K}^{\,\mathrm{dn}}(x,y). \tag{29}$$

Similarly, for $y \le x \le 0$, the Marchenko kernel Ω_r is connected to the auxiliary functions $M^{\,\mathrm{dn}}$ and $\bar{M}^{\,\mathrm{dn}}$ in this way:

$$\Omega_r(x+y) + \int_{-\infty}^x M^{\,\mathrm{up}}(x,z)\,\Omega_r(z+y)\,dz = -\bar{M}^{\,\mathrm{up}}(x,y). \tag{30}$$

As a result, assuming known the auxiliary functions, (29) and (30) can be interpreted as structured Fredholm integral equations of the second kind having the initial Marchenko kernels Ω_ℓ and Ω_r as their unknowns.

It is important to note that, from the computational point of view, each Marchenko kernel can be treated as a function of only one variable, as we only have to deal with the sum of the two variables.

4.2 The scattering matrix and the Fourier transforms of the reflection coefficients

Let us begin by recalling that, as proposed in [16], the coefficients of the scattering matrix $S(\lambda)$ can be represented as follows:

$$T(\lambda) = \frac{1}{a_{\ell 4}(\lambda)} = \frac{1}{a_{r1}(\lambda)}, \tag{31}$$

$$L(\lambda) = \frac{a_{\ell 2}(\lambda)}{a_{\ell 4}(\lambda)} = -\frac{a_{r2}(\lambda)}{a_{r1}(\lambda)}, \tag{32}$$

$$R(\lambda) = \frac{a_{r3}(\lambda)}{a_{r1}(\lambda)} = -\frac{a_{\ell 3}(\lambda)}{a_{\ell 4}(\lambda)} \tag{33}$$

where the $\{a_{\ell j}(\lambda)\}$ and the $\{a_{rj}(\lambda)\}$ denote the entries of the transition matrices from the left and from the right, respectively. More precisely,

$$\begin{cases} a_{\ell 1}(\lambda) &= 1 - \displaystyle\int_{\mathbb{R}^+} e^{-i\lambda z}\,\bar{\Phi}^{\,\mathrm{dn}}(z)dz \\ a_{\ell 2}(\lambda) &= -\displaystyle\int_{\mathbb{R}} e^{2i\lambda y} u_0(y)dy - \int_{\mathbb{R}} e^{i\lambda z}\Phi^{\,\mathrm{dn}}(z)dz \\ a_{\ell 3}(\lambda) &= \displaystyle\int_{\mathbb{R}} e^{-2i\lambda y} v_0(y)dy + \int_{\mathbb{R}} e^{-i\lambda z}\bar{\Phi}^{\,\mathrm{up}}(z)dz \\ a_{\ell 4}(\lambda) &= 1 + \displaystyle\int_{\mathbb{R}^+} e^{i\lambda z}\Phi^{\,\mathrm{up}}(z)dz, \end{cases} \tag{34}$$

where

$$\bar{\Phi}^{\,\mathrm{dn}}(z) = \int_{\mathbb{R}} u_0(y)\bar{K}^{\,\mathrm{dn}}(y, y+z)dy, \qquad \Phi^{\,\mathrm{dn}}(z) = \int_{-\infty}^{\frac{z}{2}} u_0(y)K^{\,\mathrm{dn}}(y, z-y)dy, \tag{35}$$

$$\Phi^{\text{up}}(z) = \int_{\mathbb{R}} v_0(y) K^{\text{up}}(y, y+z)dy, \qquad \bar{\Phi}^{\text{up}}(z) = \int_{-\infty}^{\frac{z}{2}} v_0(y) \bar{K}^{\text{up}}(y, z-y)dy, \tag{36}$$

and

$$\begin{cases} a_{r1}(\lambda) &= 1 + \int_{\mathbb{R}^+} e^{i\lambda z} \Psi^{\text{dn}}(z)dz \\ a_{r2}(\lambda) &= \int_{\mathbb{R}} e^{2i\lambda y} u_0(y)dy + \int_{\mathbb{R}} e^{i\lambda z} \bar{\Psi}^{\text{dn}}(z)dz \\ a_{r3}(\lambda) &= -\int_{\mathbb{R}} e^{-2i\lambda y} v_0(y)dy - \int_{\mathbb{R}} e^{-i\lambda z} \Psi^{\text{up}}(z)dz \\ a_{r4}(\lambda) &= 1 - \int_{\mathbb{R}^+} e^{-i\lambda z} \bar{\Psi}^{\text{up}}(z)dz \end{cases} \tag{37}$$

where

$$\Psi^{\text{dn}}(z) = \int_{\mathbb{R}} u_0(y) M^{\text{dn}}(y, y-z)dy, \qquad \bar{\Psi}^{\text{dn}}(z) = \int_{\frac{z}{2}}^{+\infty} u_0(y) \bar{M}^{\text{dn}}(y, z-y)dy, \tag{38}$$

$$\Psi^{\text{up}}(z) = \int_{\frac{z}{2}}^{+\infty} v_0(y) M^{\text{up}}(y, z-y)dy, \qquad \bar{\Psi}^{\text{up}}(z) = \int_{\mathbb{R}} v_0(y) \bar{M}^{\text{up}}(y, y-z)dy. \tag{39}$$

While the approximation of T simply requires the computation of $a_{\ell 4}(\lambda)$ and $a_{r1}(\lambda)$, that of ρ and ℓ is more complicated. In fact, to approximate $\rho(\alpha)$ and $\ell(\alpha)$ we first have to compute the scattering coefficients by means of (34) – (39), then the reflection coefficients $R(\lambda)$ and $L(\lambda)$ by using (33) and (32) and, finally, $\rho(\alpha)$ and $\ell(\alpha)$ by resorting to the inverse and direct Fourier transforms as indicated in (13) and (14).

The stability of this numerical procedure essentially depends on the decay of $R(\lambda)$ and $L(\lambda)$ as $\lambda \to \pm\infty$, since the smoother the initial potential the faster their decay. If the initial potential has jump discontinuities then R and L decay slowly as $\lambda \to \infty$ while if $u_0 \in C^\infty(\mathbb{R})$ then R and L decay superpolynomially.

Hence, this procedure is effective whenever the initial potential is smooth enough, that is at least $u_0 \in C(\mathbb{R})$. If this is not the case the Fourier transforms $\rho(\alpha)$ and $\ell(\alpha)$ can be approximated by solving the structured Fredholm integral equations stated in the following theorems. The development of an effective algorithm for solving these equations is devoted to a subsequent paper.

Theorem 1 *The function $\rho(\alpha)$ is the unique solution of each of the following Fredholm integral equation of the second kind :*

$$\rho(\alpha) + \int_0^\infty \Phi^{up}(z)\, \rho(z+\alpha)dz = -\frac{1}{2} v_0\left(\frac{\alpha}{2}\right) - \bar{\Phi}^{up}(\alpha), \tag{40}$$

$$\rho(\alpha) + \int_0^\infty \Psi^{dn}(z)\, \rho(z+\alpha)dz = -\frac{1}{2} v_0\left(\frac{\alpha}{2}\right) - \Psi^{up}(\alpha), \tag{41}$$

where Φ^{up} *and* $\bar{\Phi}^{up}$ *are given in* (36) *and* Ψ^{dn} *and* Ψ^{up} *are defined in* (38), (39).

Proof Let us first note that from (33)

$$a_{\ell 4}(\lambda)R(\lambda) = -a_{\ell 3}(\lambda) \tag{42}$$

where $a_{\ell 4}$ and $a_{\ell 3}$ are defined in (34). Introducing the Heaviside function $H(z) = 1$ for $z \geq 0$ and $H(z) = 0$ for $z < 0$, taking into account that

$$R(\lambda) = \mathcal{F}\{\rho(\alpha)\}$$

and using (42) we can write

$$(1 + \mathcal{F}\{\Phi^{up}(-\alpha)H(-\alpha)\})\,\mathcal{F}\{\rho(\alpha)\} = -\mathcal{F}\left\{\frac{1}{2}v_0\left(\frac{\alpha}{2}\right) + \bar{\Phi}^{up}(\alpha)\right\}.$$

Hence, applying the inverse Fourier transform and the convolution theorem, we have

$$\rho(\alpha) + (\Phi^{up}(-\alpha)H(-\alpha)) * \rho(\alpha) = -\frac{1}{2}v_0\left(\frac{\alpha}{2}\right) - \bar{\Phi}^{up}(\alpha),$$

and then the equation (40) is an immediate consequence of the convolution definition and the Heaviside function. Equation (41) can be obtained similarly, noting that $R(\lambda)$ satisfies the relation

$$a_{r1}(\lambda)R(\lambda) = a_{r3}(\lambda)$$

and that

$$a_{r1}(\lambda) = 1 + \mathcal{F}\left\{\Psi^{dn}(-\alpha)H(-\alpha)\right\} \quad \text{and} \quad a_{r3}(\lambda) = \mathcal{F}\left\{\frac{1}{2}v_0\left(\frac{\alpha}{2}\right) + \Psi^{up}(\alpha)\right\}.$$

□

We note that, from the numerical point of view, it is irrelevant if we solve (40) rather than (41), since both are Fredholm integral equations of the second kind, equally structured.

Applying the same technique we obtain the analogous

Theorem 2 *The function* $\ell(\alpha)$ *is the unique solution of the two structured Fredholm integral equations of the second kind:*

$$\ell(\alpha) + \int_0^\infty \Phi^{up}(z)\,\ell(\alpha - z)dz = -\frac{1}{2}u_0\left(\frac{\alpha}{2}\right) - \Phi^{dn}(\alpha) \tag{43}$$

$$\ell(\alpha) + \int_0^\infty \Psi^{dn}(z)\,\ell(\alpha - z)dz = -\frac{1}{2}u_0\left(\frac{\alpha}{2}\right) - \bar{\Psi}^{dn}(\alpha), \tag{44}$$

where Ψ^{dn} *and* $\bar{\Psi}^{dn}$ *are defined in* (38) *and* Φ^{dn} *and* Φ^{up} *are given in* (35), (36).

We omit the proof, as it is analogous to the previous one, after noting that $a_{\ell 4}(\lambda)L(\lambda) = a_{\ell 2}(\lambda)$ and $a_{r1}(\lambda)L(\lambda) = -a_{r2}(\lambda)$ with $L(\lambda) = \mathcal{F}\{\ell(-\alpha)\}$.

5 The numerical method

Let us now assume, for computational simplicity, that the support of the initial solution is bounded, that is

$$u_0(x) = 0, \quad \text{for} \quad |x| > L, \tag{45}$$

which can be considered acceptable whenever $u_0(x) \to 0$ for $|x| \to \infty$, provided L is taken large enough. This hypothesis, as in part already proved in [7], allows us to greatly simplify the algorithms for the computation of the auxiliary functions and also those for the computation of the Marchenko kernels and the Fourier transforms of the reflection coefficients.

The method we propose provides successively the numerical solution of:

1. the four systems (19)–(22) of Volterra integral equations for the computation of the four pairs of auxiliary functions;
2. the two Fredholm integral equations (29), (30) for the computation of the Marchenko kernels from the left and from the right Ω_ℓ and Ω_r, respectively;
3. the transition matrices from the left and from the right, the scattering matrix and then the inverse Fourier transforms ρ of the reflection coefficients from the right R and the Fourier transform ℓ of the reflection coefficient from the left L.

Once the Marchenko kernels $\Omega_\ell(\alpha)$ and $\Omega_r(\alpha)$ and the functions $\rho(\alpha)$ and $\ell(\alpha)$ have been obtained, the bound states $\{\lambda_j\}_{j=1}^n$ with their multiplicities $\{m_j\}_{j=1}^n$ and the norming constants $\{(\Gamma_\ell)_{js}, (\Gamma_r)_{js}\}$ are computed by applying to the monomial-exponential sums (9), (10) the matrix-pencil method proposed in [8] and [6].

5.1 Auxiliary functions computation

As said before, our numerical method for the solution of the Volterra systems (19)–(22) is greatly affected by the hypothesis (45). It implies a reduction of the auxiliary function supports, which allows us to develop algorithms that are simpler and numerically stable.

As proved in [7] and in the Appendix of this paper, $\bar{K}^{\text{up}}$ and $\bar{K}^{\text{dn}}$ have the supports depicted in Fig. 1. Taking into account the symmetry properties (27) or (28) of systems (19) and (20), it is immediate to check that $supp(K^{\text{up}}) = supp(\bar{K}^{\text{dn}})$ and $supp(K^{\text{dn}}) = supp(\bar{K}^{\text{up}})$.

For the numerical solution of system (19), the following properties, proved in [7], are also important:

1. If $x \le -L$, whatever h, $\bar{K}^{\text{up}}(x, y)$ and $K^{\text{dn}}(x, y)$ are both constant on the line $y = x + h$. For this reason we put $\bar{K}^{\text{up}}(x, x+h) = \mathcal{C}^{\text{up}}_{\bar{K},h}$ and $K^{\text{dn}}(x, x+h) = \mathcal{C}^{\text{dn}}_{K,h}$ for each given value h.
2. If $x < -L$ and $x + y > -2L$, $\bar{K}^{\text{dn}}(x, y)$ and $K^{\text{up}}(x, y)$ are both constant on each line $x + y = -2(L - h)$ for each $0 < h < 2L$.

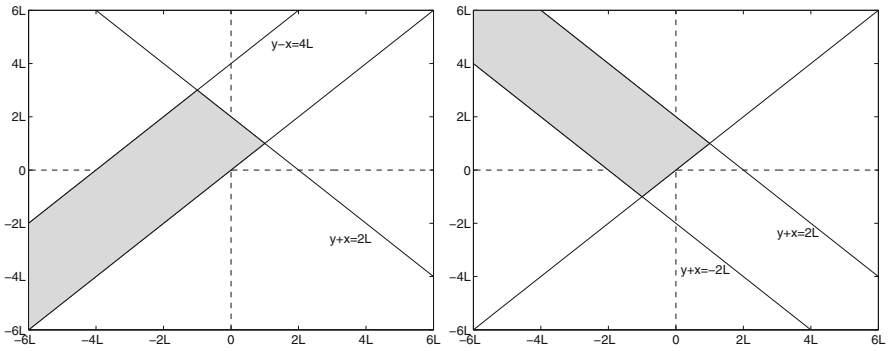

Fig. 1 Supports of the auxiliary functions $\bar{K}^{\,\mathrm{up}}$ and $K^{\,\mathrm{dn}}$ (to the *left*) and $\bar{K}^{\,\mathrm{dn}}$ and $K^{\,\mathrm{up}}$ (to the *right*)

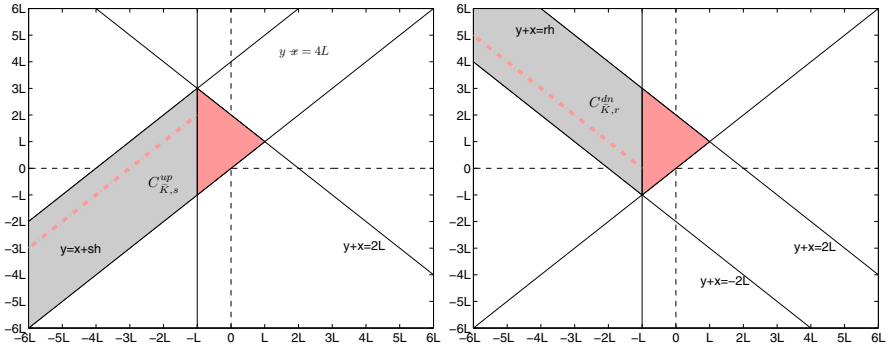

Fig. 2 Additional properties of $\bar{K}^{\,\mathrm{up}}$ and $K^{\,\mathrm{dn}}$ (to the *left*) and $\bar{K}^{\,\mathrm{dn}}$ and $K^{\,\mathrm{up}}$ (to the *right*)

These two results are graphically represented in Fig. 2, where $\bar{K}^{\,\mathrm{dn}}(x, x+h) = \mathcal{C}^{\,\mathrm{dn}}_{\bar{K},h}$ and $\bar{K}^{\,\mathrm{up}}(x, x+h) = \mathcal{C}^{\,\mathrm{up}}_{K,h}$.

Analogous considerations, based on results reported in [7] and in the Appendix, allow us to claim that the supports of $(\bar{M}^{\,\mathrm{up}}, \bar{M}^{\,\mathrm{dn}})$ are those depicted in Fig. 3. As for $(\bar{K}^{\,\mathrm{up}}, \bar{K}^{\,\mathrm{dn}})$ and $(K^{\,\mathrm{up}}, K^{\,\mathrm{dn}})$ as for the pairs $(\bar{M}^{\,\mathrm{up}}, \bar{M}^{\,\mathrm{dn}})$ and $(M^{\,\mathrm{up}}, M^{\,\mathrm{dn}})$ we have additional properties very useful from the numerical point of view. With obvious meaning of the symbols, they are reported in Fig. 4.

A simple inspection of Figs. 1 and 3 makes it evident that the area where we need to compute $\bar{K}^{\,\mathrm{up}}$ and $\bar{K}^{\,\mathrm{dn}}$, as well as $K^{\,\mathrm{up}}$ and $K^{\,\mathrm{dn}}$, is given by the orange triangle represented in Fig. 5. In the remaining areas of the respective supports their values are immediately obtained by using those of the orange triangle. The orange line shows, in particular, the values of the orange triangle we use to compute $(\bar{K}^{\,\mathrm{up}}, \bar{K}^{\,\mathrm{dn}})$ and $(K^{\,\mathrm{up}}, K^{\,\mathrm{dn}})$ in the point of the gray area. Similar considerations hold true for the computational area of the pairs $(\bar{M}^{\,\mathrm{up}}, \bar{M}^{\,\mathrm{dn}})$ and $(M^{\,\mathrm{up}}, M^{\,\mathrm{dn}})$ which is depicted in Fig. 6, with the analogous meaning of the symbols.

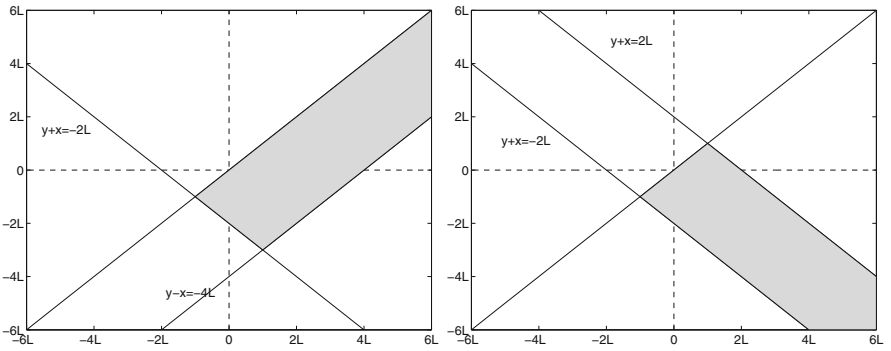

Fig. 3 Supports of the auxiliary functions M^{up} and $\bar{M}^{\text{dn}}$ (to the *left*) and M^{dn} and $\bar{M}^{\text{up}}$ (to the *right*)

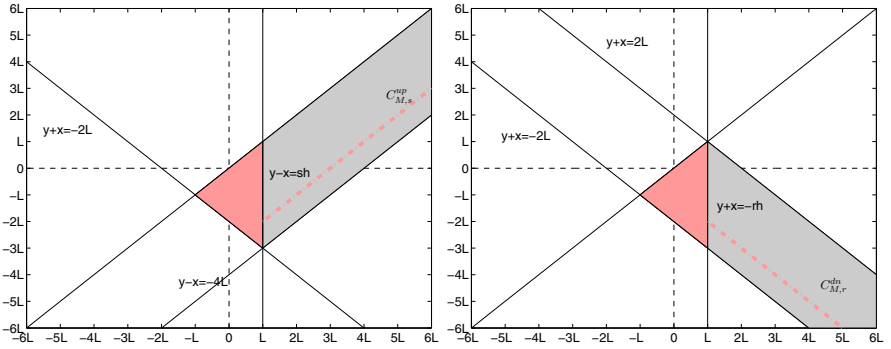

Fig. 4 Additional properties of M^{up} and $\bar{M}^{\text{dn}}$ (to the *left*) and M^{dn} and $\bar{M}^{\text{up}}$ (to the *right*)

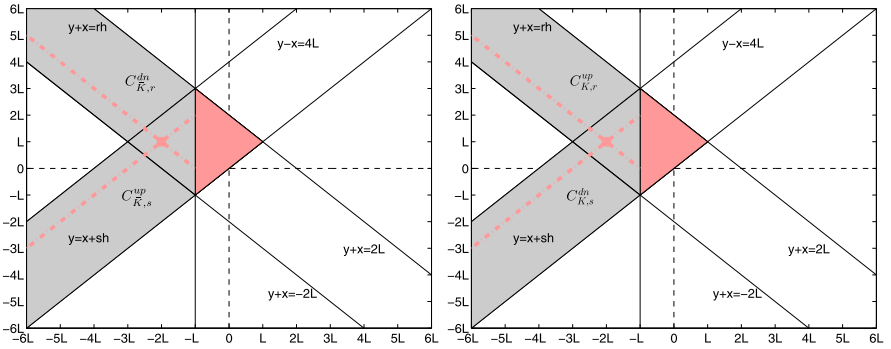

Fig. 5 Geometrical visualization of the computational area of $\bar{K}^{\text{up}}$ and $\bar{K}^{\text{dn}}$ (to the *left*) and K^{up} and K^{dn} (to the *right*)

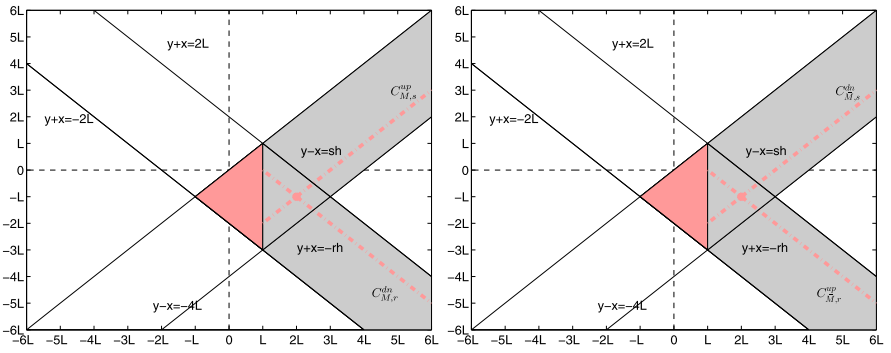

Fig. 6 Geometrical visualization of the computational area of $\bar{M}^{\,\mathrm{up}}$ and $\bar{M}^{\,\mathrm{dn}}$ (to the *left*) and $M^{\,\mathrm{up}}$ and $M^{\,\mathrm{dn}}$ (to the *right*)

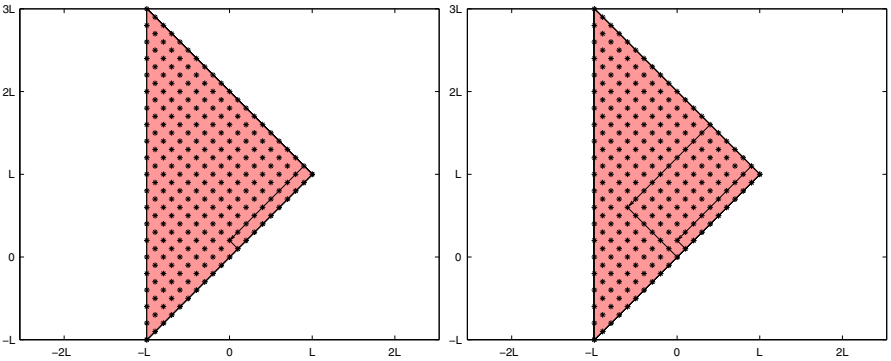

Fig. 7 Sorting visualization of collocation points in the *triangle* of $\bar{K}^{\,\mathrm{up}}$, $\bar{K}^{\,\mathrm{dn}}$, $K^{\,\mathrm{up}}$ and $K^{\,\mathrm{dn}}$

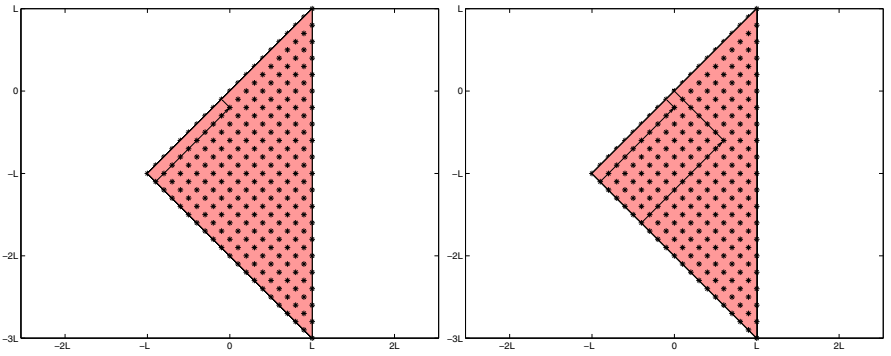

Fig. 8 Sorting visualization of collocation points in the *triangle* of $\bar{M}^{\,\mathrm{up}}$, $\bar{M}^{\,\mathrm{dn}}$, $M^{\,\mathrm{up}}$ and $M^{\,\mathrm{dn}}$

Algorithm

Given the initial solution u_0 and $v_0 = u_0^*$ in the focusing case or $v_0 = -u_0^*$ in the defocusing case, we have to solve the Volterra systems (19)–(22).

Let us start with the numerical solution of system (19). As noted before, under the hypothesis (45), we can limit ourselves to solving this system in the triangular computational area represented in Fig. 5, as the values of $\bar{K}^{\text{up}}$ and $\bar{K}^{\text{dn}}$ in the remaining parts of their support are then automatically known (Figs. 2, 4).

The algorithm that we propose in this paper is more effective that the one reported in [7] whose aim was simply to check the effectiveness of our approach, highlighting the mathematical problems to overcome to obtain a satisfactory solution of the problem. Though the collocation strategy, shown in Figs. 7, 8, is the same as used in [7], the algorithm used here is more complex and effective. In fact, it is based on the combined use of the trapezoidal rule, the composite Simpson quadrature formula and the 3/8 Simpson quadrature rule [13, Section 3.1], instead of only the composite trapezoidal quadrature formula used there.

The first step is to fix a proper mesh in the computational area which can be done by fixing $n \in \mathbb{N}$, taking $h = \frac{L}{n}$ and introducing the following mesh points:

$$\mathcal{D}_k = \{(x_i, x_{i+2k}), \qquad x_i = ih, \quad i = n-k, n-k-1, \ldots, -n+1, -n\}$$

where the index $k = 0, \ldots, 2n$ identifies the line $y = x + 2kh$ on which we want to compute the unknown functions, whereas i labels the abscissa of the ith mesh point on the line.

For the sake of simplicity, let us hereafter write u and v in place of u_0 and v_0, respectively. The computational strategy requires us to compute first $\bar{K}^{\text{up}}$ and $\bar{K}^{\text{dn}}$ in the nodal points of the bisector (x_i, x_i). Consequently, recalling (23) and denoting by $\bar{K}^{\text{up}}_{r,s}$, $\bar{K}^{\text{dn}}_{r,s}$ the approximation of $\bar{K}^{\text{up}}(x, y)$, $\bar{K}^{\text{dn}}(x, y)$ in the nodal points of $\mathcal{D}_0$, we can write

$$\bar{K}^{\text{up}}_{i,i} = -\frac{1}{2}\int_{x_i}^{\infty} u(z)v(z)\,dz = -\frac{1}{2}\int_{x_i}^{x_{n+1}} u(z)v(z)\,dz$$
$$\bar{K}^{\text{dn}}_{i,i} = \frac{1}{2}v_i, \qquad i = n, n-1, \ldots, -n+1, -n.$$

To approximate the above integral, it is convenient to use different quadrature formulae, according to the node x_i. More precisely for:

- $i = n$, being involved only two nodal points, we use the trapezoidal rule

$$\bar{K}^{\text{up}}_{i,i} = -\frac{h}{4}\{u_n v_n + u_{n+1}v_{n+1}\} = -\frac{h}{4}u_n v_n$$

  as, for (23), $u_{n+1}v_{n+1} = 0$;
- $i = n-\ell$, $\ell = 1, 3, 5, \ldots, 2n-1$, we apply the composite Simpson rule. Recalling that $u_{n+1} = v_{n+1} = 0$, we then obtain

$$\bar{K}^{\text{up}}_{i,i} = \frac{h}{3}\left[u_i v_i + 4\sum_{j=1}^{\frac{\ell+1}{2}} u_{i+2j-1}v_{i+2j-1} + 2\sum_{j=1}^{\frac{\ell+1}{2}-1} u_{i+2j}v_{i+2j}\right];$$

- $i = n - \ell$, $\ell = 2, 4, 6, \ldots, 2n$, noting that

$$\int_{x_i}^{x_{n+1}} u(z)v(z)\,dz = \left\{\int_{x_i}^{x_{i+3}} + \int_{x_{i+3}}^{x_{n+1}}\right\} u(z)v(z)dz,$$

and that the first integral involves four nodes, while the second integral involves an odd number of nodes, we can apply the 3/8 Simpson rule [13, p. 128] for computing the first integral and the composite Simpson quadrature formula for the second one. Hence, recalling again that $u_{n+1} = v_{n+1} = 0$, we have

$$\begin{aligned}\bar{K}^{\,\mathrm{up}}_{i,i} =& \frac{3}{8}h\left[u_i v_i + 3u_{i+1}v_{i+1} + 3u_{i+2}v_{i+2} + u_{i+3}v_{i+3}\right] \\ &+ \frac{h}{3}\left[u_{i+3}v_{i+3} + 4\sum_{j=1}^{\frac{\ell}{2}} u_{i+2+2j} + 2\sum_{j=1}^{\frac{\ell}{2}-1} u_{i+3+2j}v_{i+3+2j}\right].\end{aligned}$$

Once $\bar{K}^{\,\mathrm{up}}$ and $\bar{K}^{\,\mathrm{dn}}$ on the nodal points of the bisector $y = x$ are known, to evaluate them on the nodal points of the parallel lines to the bisector, we collocate system (19) on the nodes of the mesh (x_i, x_{i+2k}), taking successively $k = 1, \ldots, 2n$ and, fixing k, assuming $i = n - k, \ldots, -n + 1, -n$. Hence, we can write

$$\begin{cases}\bar{K}^{\,\mathrm{up}}_{i,i+2k} + \displaystyle\int_{x_i}^{\infty} u(z)\,\bar{K}^{\,\mathrm{dn}}(z, z + 2kh)\,dz = 0, \\ \bar{K}^{\,\mathrm{dn}}_{i,i+2k} - \displaystyle\int_{x_i}^{x_{i+k}} v(z)\,\bar{K}^{\,\mathrm{up}}(z, 2(i+k)h - z)\,dz = \frac{1}{2}v_{i+k}.\end{cases}$$

These formulae, taking into account the support of the functions involved (Fig. 5), reduce to

$$\begin{cases}\bar{K}^{\,\mathrm{up}}_{i,i+2k} + \displaystyle\int_{x_i}^{x_{n-k+1}} u(z)\,\bar{K}^{\,\mathrm{dn}}(z, z + 2kh)\,dz = 0, \\ \bar{K}^{\,\mathrm{dn}}_{i,i+2k} - \displaystyle\int_{x_i}^{x_{i+k}} v(z)\,\bar{K}^{\,\mathrm{up}}(z, 2(i+k)h - z)\,dz = \frac{1}{2}v_{i+k}.\end{cases}$$

To compute the first integral

$$I^1_{k,i} = \int_{x_i}^{x_{n-k+1}} u(z)\,\bar{K}^{\,\mathrm{dn}}(z, z + 2kh)\,dz$$

we use different quadrature formulae, according to the node x_i. More precisely, fixing k, for:

- $i = n - k$, being involved only two nodal points, we use the trapezoidal rule and then take

$$I^1_{k,i} = \frac{h}{2}\left\{u_{n-k}\bar{K}^{\,\mathrm{dn}}_{n-k,n+k} + u_{n-k}\bar{K}^{\,\mathrm{dn}}_{n-k+1,n+k+1}\right\} = \frac{h}{2}u_{n-k}\bar{K}^{\,\mathrm{dn}}_{n-k,n+k},$$

  as the nodal point (x_{n-k+1}, x_{n+k+1}) is outside the support of $\bar{K}^{\,\mathrm{dn}}(x, y)$;
- $i = n - k - \ell$, with ℓ odd and $\ell \le 2n - k$, applying the composite Simpson's rule, we obtain

$$I^1_{k,i} = \frac{h}{3}\left[u_i\bar{K}^{\,\mathrm{dn}}_{i,i+2k} + 4\sum_{j=1}^{\frac{\ell+1}{2}} u_{i+2j-1}\bar{K}^{dn}_{i+2j-1,i+2j-1+2k} + 2\sum_{j=1}^{\frac{\ell+1}{2}} u_{i+2j-1}\bar{K}^{dn}_{i+2j,i+2j+2k}\right],$$

  as $\bar{K}^{\,\mathrm{dn}}_{n-k+1,n+k+1} = 0$.
- $i = n - k - \ell$, with ℓ even and $\ell \le 2n - k$, noting that

$$I^1_{k,i} = \left\{\int_{x_i}^{x_{i+3}} + \int_{x_{i+3}}^{x_{n-k+1}}\right\} u(z)\,\bar{K}^{\,\mathrm{dn}}(z, z + 2kh)\,dz,$$

  we apply the 3/8 Simpson's rule for the first integral and the composite Simpson's quadrature formula for the second one. Hence, we have

$$\begin{aligned} I^1_{k,i} = {} & \frac{3}{8}h\left[u_i\bar{K}^{\,\mathrm{dn}}_{i,i+2k} + 3u_{i+1}\bar{K}^{\,\mathrm{dn}}_{i+1,i+1+2k} + 3u_{i+2}\bar{K}^{\,\mathrm{dn}}_{i+2,i+2+2k} + u_{i+3}\bar{K}^{\,\mathrm{dn}}_{i+3,i+3+2k}\right] \\ & + \frac{h}{3}\left[u_{i+3}\bar{K}^{\,\mathrm{dn}}_{i+3,i+3+2k} + 4\sum_{j=1}^{\frac{\ell}{2}} u_{i+2+2j}\bar{K}^{\,\mathrm{dn}}_{i+2+2j,i+2+2j+2k}\right. \\ & \left. + 2\sum_{j=1}^{\frac{\ell}{2}-1} u_{i+3+2j}\bar{K}^{\,\mathrm{dn}}_{i+3+2j,i+3+2j+2k}\right] \end{aligned}$$

  as the nodal point (x_{n-k+1}, x_{n+k+1}) is outside the support of $\bar{K}^{\,\mathrm{dn}}(x, y)$.

The computation of the second integral

$$I^2_{k,i} = \int_{x_i}^{x_{i+k}} v(z)\,\bar{K}^{\,\mathrm{up}}(z, 2(i + k)h - z)\,dz,$$

is also based on the use of quadrature formulae, essentially dependent on the line $y = x + 2kh$. More precisely, for:

- $k = 1$, as only two nodal points are involved, we apply the trapezoidal rule, obtaining

$$I^2_{k,i} = \frac{h}{2}\left\{v_i\bar{K}^{\,\mathrm{up}}_{i,i+2} + v_{i+1}\bar{K}^{\,\mathrm{up}}_{i+1,i+1}\right\};$$

- $k = 2, 4, 6, \ldots, 2n$, we use the composite Simpson quadrature formula. Proceeding in this way we obtain for $i = n - k, \ldots, -n$

$$\begin{aligned} I^2_{k,i} =& \frac{h}{3}\left[v_i \bar{K}^{\text{up}}_{i,i+2k} + 4\sum_{j=1}^{\frac{\ell}{2}} v_{i+2j-1} \bar{K}^{\text{up}}_{i+2j-1,i-2j+1+2k} \right. \\ & \left. + 2\sum_{j=1}^{\frac{\ell}{2}-1} v_{i+2j} \bar{K}^{\text{up}}_{i+2j,i-2j+2k} + v_{i+k} \bar{K}^{\text{up}}_{i+k,i+k} \right] \\ =& \frac{h}{3} v_i \bar{K}^{\text{up}}_{i,i+2k} + w_{k,i}, \end{aligned}$$

  where $w_{k,i}$ is the sum of the $\bar{K}^{\text{up}}$ values in the nodal points belonging to the bisector and the previous parallels. In fact, the $\bar{K}^{\text{up}}$ values of the first sum belong to the lines $y = x + [2k - 2(2j - 1)]h$, those of the second one belong to the lines $y = x + [2k - 4j]h$ and the last term to $y = x$.
- $k = 3, 5, 7, \ldots, 2n - 1$, we write

$$I^2_{k,i} = \left\{ \int_{x_i}^{x_{i+3}} + \int_{x_{i+3}}^{x_{i+k}} \right\} v(z)\, \bar{K}^{\text{up}}(z, 2(i+k)h - z)\, dz$$

  and then we use the 3/8 Simpson rule for the first integral and again the composite Simpson quadrature formula for the second one:

$$\begin{aligned} I^2_{k,i} =& \frac{3}{8}h\left[v_i \bar{K}^{\text{up}}_{i,i+2k} + 3v_{i+1} \bar{K}^{\text{up}}_{i+1,i+2k-1} + 3v_{i+2} \bar{K}^{\text{up}}_{i+2,i+2k-2} + v_{i+3} \bar{K}^{\text{up}}_{i+3,i+2k-3} \right] \\ & + \frac{h}{3}\left[v_{i+3} \bar{K}^{\text{up}}_{i+3,i+2k-3} + 4\sum_{j=1}^{\frac{\ell}{2}} v_{i+2+2j} \bar{K}^{\text{up}}_{i+2+2j,i-2-2j+2k} \right. \\ & \left. + 2\sum_{j=1}^{\frac{\ell}{2}-1} u_{i+3+2j} \bar{K}^{\text{up}}_{i+3+2j,i-3-2j+2k} + v_{i+k} \bar{K}^{\text{up}}_{i+k,i+k} \right] \\ =& \frac{3}{8}h v_i \bar{K}^{\text{up}}_{i,i+2k} + w_{k,i}, \end{aligned}$$

  where $w_{k,i}$ is known, being a linear combination of $\bar{K}^{\text{up}}$ values already computed. Once the integrals have been approximated as described above, we obtain the $2n$ following structured systems of order $2(2n + 1 - k)$, $k = 1, \ldots, 2n$

$$\begin{cases} \bar{\mathbf{k}}^{\text{up}}_k + \mathbf{U}_{k,1} \bar{\mathbf{k}}^{\text{dn}}_k = \mathbf{0} \\ \mathbf{U}_{k,2} \bar{\mathbf{k}}^{\text{up}}_k + \bar{\mathbf{k}}^{\text{dn}}_k = \mathbf{v}_k - \mathbf{w}_k \end{cases} \tag{46}$$

that allow us to compute the functions $\bar{K}^{\text{up}}$ and $\bar{K}^{\text{dn}}$ in the $2n+1-k$ nodal points of $\mathcal{D}_k$ as

$$\bar{\mathbf{k}}_k^{\text{up}} = \left(\bar{K}^{\text{up}}_{n-k,n+k}, \bar{K}^{\text{up}}_{n-k-1,n+k-1}, \ldots, \bar{K}^{\text{up}}_{-n+1,-n+2k+1}, \bar{K}^{\text{up}}_{-n,-n+2k}\right)^T$$
$$\bar{\mathbf{k}}_k^{\text{dn}} = \left(\bar{K}^{\text{dn}}_{n-k,n+k}, \bar{K}^{\text{dn}}_{n-k-1,n+k-1}, \ldots, \bar{K}^{up}_{-n+1-n+2k+1}, \bar{K}^{\text{dn}}_{-n,-n+2k}\right)^T.$$

Notice that $\mathbf{U}_{k,1}$, $\mathbf{U}_{k,2}$ are the following structured matrices:

$$\mathbf{U}_{k,2} = -c_k h\, diag(v_{n-k},\ v_{n-k-1}, \ldots, v_{-n+1}, v_{-n})$$

with $c_1 = 1/2$, $c_2 = c_4 = \cdots = c_{2n} = 1/3$ and $c_3 = c_5 = \cdots = c_{2n-1} = 3/8$ and $\mathbf{U}_{k,1}$ is the following nonsingular lower triangular matrix

$$\mathbf{U}_{k,1} = h\, \tilde{\mathbf{U}}_{k,1} diag(u_{n-k},\ u_{n-k-1}, \ldots, u_{-n+1}, u_{-n})$$

where the rows of the matrix $\tilde{\mathbf{U}}_{k,1}$ are defined as follows:

$$(\tilde{\mathbf{U}}_{k,1})_1 = \left(\frac{1}{2}\, 0\, 0 \ldots 0\, 0\, 0\right)$$
$$(\tilde{\mathbf{U}}_{k,1})_2 = \left(\frac{4}{3}\, \frac{1}{3}\, 0\, 0 \ldots 0\, 0\, 0\right)$$
$$(\tilde{\mathbf{U}}_{k,1})_3 = \left(\frac{9}{8}\, \frac{9}{8}\, \frac{3}{8}\, 0\, 0 \ldots 0\, 0\, 0\right)$$
$$(\tilde{\mathbf{U}}_{k,1})_{2i} = \left(\frac{4}{3}\, \frac{2}{3}\, \frac{4}{3}\, \frac{2}{3} \cdots \frac{4}{3}\, \frac{1}{3}\, 0\, 0 \ldots 0\, 0\, 0\right) \quad i \geq 2$$
$$(\tilde{\mathbf{U}}_{k,1})_{2i+1} = \left(\frac{4}{3}\, \frac{2}{3}\, \frac{4}{3}\, \frac{2}{3} \cdots \frac{4}{3}\, \frac{2}{3}\, \frac{1}{3}\, \left(\frac{1}{3}+\frac{3}{8}\right)\, \frac{9}{8}\, \frac{9}{8}\, \frac{3}{8}\, 0\, 0 \ldots 0\, 0\, 0\right) \quad i \geq 2.$$

The most obvious computational strategy is to reduce (46) to a sequence of $n-k$ systems of order two. However, our numerical experiments indicate that the numerical stability increases by using a suitable iterative method.
It requires solving iteratively the system

$$(\mathbf{I} - \mathbf{U}_{k,1}\mathbf{U}_{k,2})\, \bar{\mathbf{k}}_k^{\text{up}} = \mathbf{U}_{k,1}\, \mathbf{w}_k, \tag{47}$$

and then computing

$$\bar{\mathbf{k}}_k^{\text{dn}} = \mathbf{v}_k - \mathbf{U}_{k,2}\, \bar{\mathbf{k}}_k^{\text{up}}. \tag{48}$$

The matrix of system (47), for h small enough, is diagonally dominant as each nonzero element of $\mathbf{U}_{k,1}\mathbf{U}_{k,2}$ contains a factor h^2, so that the Gauss-Seidel method is a suitable choice of iteration method, assuming as an initial vector the values of $\bar{\mathbf{k}}_k^{\text{up}}$ in the previous parallel, that is taking in the $(k+1)$th parallel to the bisector

$$(\bar{\mathbf{k}}_{k+1}^{\text{up}})^{(0)} = \bar{\mathbf{k}}_k^{\text{up}} \qquad k = 0, 1, \ldots, 2n-1. \tag{49}$$

As $\mathbf{I}-\mathbf{U}_{k,1}\mathbf{U}_{k,2}$ is lower triangular, it is of course possible to solve it by a descending technique.

Remark 3 Once we have solved system (19) we can immediately deduce the solution of system (20) taking into account Remark 1. In any case, we note that, as the computational area of system (19) is the same as that of (20), the algorithm to solve (20) is analogous to that adopted for system (19).

The same comparative considerations hold true for the computation of $(\bar{M}^{\,\mathrm{up}}, \bar{M}^{\,\mathrm{dn}})$ and $(M^{\,\mathrm{up}}, M^{\,\mathrm{dn}})$ in the nodal points of their computational area. Moreover, although the computational area for $(\bar{M}^{\,\mathrm{up}}, \bar{M}^{\,\mathrm{dn}})$ is not the same as that for $(\bar{K}^{\,\mathrm{up}}, \bar{K}^{\,\mathrm{dn}})$, the technique for their computation is essentially the same.

Noting that (Figs. 5, 6) the two computational areas are symmetric with respect to each other, we first have to compute $(\bar{M}^{\,\mathrm{up}}, \bar{M}^{\,\mathrm{dn}})$ in the bisector and then on the parallel lines $y = x - 2kh$, $k = 1, 2, \ldots, 2n$. Furthermore, to compute $\bar{M}^{\,\mathrm{dn}}$ in the bisector we can adopt the same algorithm for $\bar{K}^{\,\mathrm{up}}$ as relations (23) and (26) indicate. A comparison between the systems (19) and (21) also suggests to approximate the first integral in (21) by a simple adaptation of the method developed for the second one in (19), as well as the second integral of (21) by adapting the method for the first integral of (19).

5.2 Marchenko kernel computation

To compute Ω_ℓ and Ω_r, that is to solve the integral equations (29) and (30), we first note that (45) implies the boundedness of their supports. In fact, as proved in [7, Lemma 5.1], (45) implies that

$$supp(\Omega_\ell) \subset [0,\ 2L], \quad and \quad supp(\Omega_r) \subset [-2L,\ 0].$$

For the approximation of Ω_ℓ we collocate (29) in the nodal points

$$\{(x_{n-2i}, x_n), \quad x_{n-2i} = (n-2i)h, \quad i = 0, 1, \ldots, n\},$$

to obtain

$$\Omega_\ell(x_{2(n-i)}) + \int_{x_{n-2i}}^{x_n} K^{\,\mathrm{dn}}(x_{n-2i}, z)\Omega_\ell(z + x_n)dz = -\bar{K}^{\,\mathrm{dn}}(x_{(n-2i)}, x_n). \tag{50}$$

Now, to compute the above integral we use different quadrature formula by adopting a steplength $\delta = 2h$ that is twice the one considered in the numerical solution of system (20) to avoid the interpolation among the values of the auxiliary functions computed before. More precisely, for

- $i = 0$ we immediately obtain that

$$\Omega_{\ell,2n} = -\bar{K}^{\,\mathrm{dn}}_{n,n} = -\frac{1}{2}v_n$$

in virtue of (23);

- $i = 1$ we use the trapezoidal rule to get

$$\left(1 + \frac{\delta}{2} K^{\mathrm{dn}}_{n-2,n-2}\right) \Omega_{\ell,2(n-1)} = -\bar{K}^{\mathrm{dn}}_{n-2,n} - K^{\mathrm{dn}}_{n-2,n} \Omega_{\ell,2n};$$

- $i = 2, 4, 6, \ldots$ we use the Simpson quadrature formula

$$\begin{aligned}\left(1 + \frac{\delta}{3} K^{\mathrm{dn}}_{n-2i,n-2i}\right) \Omega_{\ell,2(n-i)} &= -\bar{K}^{\mathrm{dn}}_{n-2i,n} \\ &- \frac{\delta}{3}\left(4 \sum_{j=1}^{\frac{i+1}{2}} K^{\mathrm{dn}}_{n-2i,n-2(i-j)} \Omega_{\ell,2(n-2(i-j))}\right. \\ &\left. +2 \sum_{j=1}^{\frac{i+1}{2}-1} K^{\mathrm{dn}}_{n-2i,n-2(i-j-1)} \Omega_{\ell,2(n-(i-j-1))} + K^{\mathrm{dn}}_{n-2i,n} \Omega_{\ell,2n}\right);\end{aligned}$$

- $i = 3, 5, 7, \ldots$ as we can write

$$\begin{aligned}&\int_{x_{n-2i}}^{x_n} K^{\mathrm{dn}}(x_{n-2i}, z) \Omega_\ell(z + x_n) dz \\ &= \left\{\int_{x_{n-2i}}^{x_{n-2(i-3)}} + \int_{x_{n-2(i-3)}}^{x_n}\right\} K^{\mathrm{dn}}(x_{n-2i}, z) \Omega_\ell(z + x_n) dz\end{aligned}$$

we approximate the first integral by using the 3/8 Simpson rule and the last integral by adopting the composite Simpson quadrature formula. Hence we get

$$\begin{aligned}\left(1 + \frac{3\delta}{8} K^{\mathrm{dn}}_{n-2i,n-2i}\right) \Omega_{\ell,2(n-i)} &= -\bar{K}^{\mathrm{dn}}_{n-2i,n} - \frac{3\delta}{8}\left(3K^{\mathrm{dn}}_{n-2i,n-2(i-1)} \Omega_{\ell,2(n-(i-1))}\right. \\ &\left. + 3K^{\mathrm{dn}}_{n-2i,n-2(i-2)} \Omega_{\ell,2(n-(i-2))} + K^{\mathrm{dn}}_{n-2i,n-2(i-3)} \Omega_{\ell,2(n-(i-3))}\right) \\ &- \frac{\delta}{3}\left(K^{\mathrm{dn}}_{n-2i,n-2(i-3)} \Omega_{\ell,2(n-(i-3))} + 4 \sum_{j=1}^{\frac{i+1}{2}} K^{\mathrm{dn}}_{n-2i,n-2(2i-3-j)} \Omega_{\ell,2(n-(2i-3-j))}\right. \\ &\left. + 2 \sum_{j=1}^{\frac{i+1}{2}-1} K^{\mathrm{dn}}_{n-2i,n-2(2i-4-j)} \Omega_{\ell,2(n-(2i-4-j))} + K^{\mathrm{dn}}_{n-2i,n} \Omega_{\ell,2n}\right).\end{aligned}$$

An analogous procedure can be applied to approximate Ω_r in $[-2L, 0]$. More precisely, we collocate (30) in the nodal points

$$\{(x_{2i-n}, x_{-n}), \quad x_{2i-n} = (2i - n)h, \quad i = 0, 1, \ldots, n\},$$

to obtain

$$\Omega_r(x_{2(i-n)}) + \int_{x_{-n}}^{x_{2i-n}} M^{\text{up}}(x_{2i-n}, z)\Omega_\ell(z + x_{-n})dz = -\bar{M}^{\text{up}}(x_{(2i-n)}, x_{-n}). \quad (51)$$

Hence, by adopting the technique illustrated above,

- for $i = 0$ we immediately obtain

$$\Omega_{r,-2n} = -\bar{M}^{\text{up}}_{-n,-n} = -\frac{1}{2}u_{-n}$$

  in virtue of (23);
- for $i = 1$ we obtain

$$\left(1 + \frac{\delta}{2}M^{\text{up}}_{2-n,2-n}\right)\Omega_{r,2(1-n)} = -\bar{M}^{\text{up}}_{2-n,-n} - M^{\text{up}}_{2-n,-n}\Omega_{r,-2n};$$

- for $i = 2, 4, 6, \ldots$ we obtain

$$\begin{aligned}\left(1 + \frac{\delta}{3}M^{\text{up}}_{2i-n,2i-n}\right)\Omega_{r,2(i-n)} &= -\bar{M}^{\text{up}}_{2i-n,-n} \\ &- \frac{\delta}{3}\left(4\sum_{j=1}^{\frac{i+1}{2}} M^{\text{up}}_{2i-n,2(i-j)-n}\Omega_{r,2((i-j)-n)}\right. \\ &\left.+2\sum_{j=1}^{\frac{i+1}{2}-1} M^{\text{up}}_{2i-n,2(i-j-1)-n}\Omega_{r,2((i-j-1)-n)} + M^{\text{up}}_{2i-n,-n}\Omega_{r,-2n}\right);\end{aligned}$$

- for $i = 3, 5, 7, \ldots$ as we can write

$$\begin{aligned}&\int_{x_{-n}}^{x_{2i-n}} M^{\text{up}}(x_{2i-n}, z)\Omega_r(z + x_{-n})dz \\ &= \left\{\int_{x_{-n}}^{x_{2(i-3)-n}} + \int_{x_{2(i-3)-n}}^{x_{2i-n}}\right\} M^{\text{up}}(x_{2i-n}, z)\Omega_r(z + x_{-n})dz,\end{aligned}$$

we approximate the first integral by using the composite Simpson rule and the second one by adopting the 3/8 Simpson's quadrature formula. Hence we get

$$\left(1+\frac{3\delta}{8}M^{\text{up}}_{2i-n,2i-n}\right)\Omega_{r,2(i-n)} = -\bar{M}^{\text{up}}_{2i-n,-n} - \frac{3\delta}{8}\left(3M^{\text{up}}_{2i-n,2(i-1)-n}\Omega_{r,2((i-1)-n)} + 3M^{\text{up}}_{2i-n,2(i-2)-n}\Omega_{r,2((i-2)-n)} + M^{\text{up}}_{2i-n,2(i-3)-n}\Omega_{r,2((i-3)-n)}\right) - \frac{\delta}{3}\left(M^{\text{up}}_{2i-n,2(i-3)-n}\Omega_{r,2((i-3)-n)} + 4\sum_{j=1}^{\frac{i+1}{2}} M^{\text{up}}_{2i-3,2(2i-3-j)-n}\Omega_{r,2((2i-3-j)-n)} + 2\sum_{j=1}^{\frac{i+1}{2}-1} M^{\text{up}}_{n-2i,2(2i-4-j)-n}\Omega_{r,2((2i-4-j)-n)} + M^{\text{up}}_{2i-n,-n}\Omega_{r,-2n}\right).$$

5.3 Computation of the scattering matrix and inverse Fourier transforms of reflection coefficients

In this section we illustrate our method to approximate the scattering matrix, that is to compute the transmission coefficients T defined in (31) and the reflection coefficients R and L introduced in (32), (33). Under the additional assumption that $u_0 \in C(\mathbb{R})$, which is our working hypothesis, the function ρ and ℓ given in (13), (14) are computed by resorting to the inverse and direct discrete Fourier transform.

Approximation of the transmission coefficient T

It is based on the two equivalent definitions of the transmission coefficient

$$T(\lambda) = \frac{1}{a_{\ell 4}(\lambda)}, \qquad T(\lambda) = \frac{1}{a_{r1}(\lambda)} \tag{52}$$

that is on the computation of the coefficients of the transition matrices

$$a_{\ell 4}(\lambda) = 1 + \int_{\mathbb{R}^+} e^{i\lambda z}\Phi^{\text{up}}(z)dz = 1 + 2\pi\mathcal{F}^{-1}\left\{\Phi^{\text{up}}(\lambda)H(\lambda)\right\}, \tag{53}$$

$$a_{r1}(\lambda) = 1 + \int_{\mathbb{R}^+} e^{i\lambda z}\Psi^{\text{dn}}(z)dz = 1 + 2\pi\mathcal{F}^{-1}\left\{\Psi^{\text{dn}}(\lambda)H(\lambda)\right\}, \tag{54}$$

where H denotes the Heaviside function and $\mathcal{F}^{-1}\{g\}$ stands for the inverse Fourier transform of g.

Let us only illustrate the algorithm for the computation of the coefficient $a_{\ell 4}$ as the computation of a_{r1} is analogous.

At first we note that, taking into account (45) and the support of K^{up}, the kernel Φ^{up} of (40) can be written as follows:

$$\Phi^{\text{up}}(z) = \begin{cases} \displaystyle\int_{-L}^{L-\frac{z}{2}} v_0(y) K^{\text{up}}(y, y+z)dy, & \text{for} \quad 0 \le z \le 4L \\ 0, & \text{for} \quad z > 4L. \end{cases} \tag{55}$$

Then, writing, for simplicity, $\Phi_j^{\text{up}} = \Phi^{\text{up}}(z_j) = \Phi^{\text{up}}(2hj),\ j = 0, 1, 2, \ldots, 2n-1$ we have successively to compute $\Phi_0^{\text{up}},\ \Phi_1^{\text{up}}, \ldots, \Phi_{2n-1}^{\text{up}}$ to obtain

$$\Phi_j^{\text{up}} = \int_{-nh}^{(n-j)h} v_0(y) K^{\text{up}}(y, y+2hj)dy, \quad j = 0, 1, \ldots, 2n-1.$$

We remark that its computation requires only the values of $K^{\text{up}}(y, y+2hj)$ which we have already computed since they are the values of K^{up} on the jth parallel to the bisector $y = x$. For this reason Φ_j^{up} can be computed by simply adopting the computational strategy that we developed for computing K^{up}. At this point the approximation of $T(\lambda)$, easily follows by using (52).

Approximation of the reflection coefficients R and L

In the matter of the computation of the reflection coefficients, taking into account (33) and (32), we can write

$$R(\lambda) = -T(\lambda)\, a_{\ell 3}(\lambda), \qquad L(\lambda) = T(\lambda)\, a_{\ell 2}(\lambda) \tag{56}$$

where $T(\lambda) = \dfrac{1}{a_{\ell 4}(\lambda)}$,

$$a_{\ell 3}(\lambda) = \int_{\mathbb{R}} e^{-i\lambda y} \left[\frac{1}{2} v_0\left(\frac{y}{2}\right) + \bar{\Phi}^{\text{up}}(y) \right] dy = \mathcal{F}\left\{ \frac{1}{2} v_0\left(\frac{y}{2}\right) + \bar{\Phi}^{\text{up}}(y) \right\},$$

and

$$a_{\ell 2}(\lambda) = -\int_{\mathbb{R}} e^{i\lambda y} \left(\frac{1}{2} u_0\left(\frac{y}{2}\right) + \Phi^{\text{dn}}(y) \right) dy = -2\pi \mathcal{F}^{-1}\left\{ \frac{1}{2} u_0\left(\frac{y}{2}\right) + \Phi^{\text{dn}}(y) \right\}.$$

Other equivalent expressions can be deducted by using the definitions of R, L and T in terms of the coefficients of the transmission matrix from the right.

To approximate $a_{\ell 3}$, taking into account (45) and the support of $\bar{K}^{\text{up}}$, first we note that

$$\bar{\Phi}^{\text{up}}(z) = \begin{cases} \displaystyle\int_{-L}^{\frac{z}{2}} v_0(y) \bar{K}^{\text{up}}(y, z-y)dy, & \text{for} \quad |z| \le 2L \\ 0, & \text{for} \quad |z| > 2L. \end{cases} \tag{57}$$

Moreover, adopting the notation used before and noting that $\bar{\Phi}^{\text{up}}_{-n} = \bar{\Phi}^{\text{up}}(-n) = \bar{\Phi}^{\text{up}}(-2nh) = 0$, we can write

$$\bar{\Phi}^{\text{up}}_i = \int_{-nh}^{ih} v_0(y)\bar{K}^{\text{up}}(y, 2hi - y)dy, \quad i = -n+1, \ldots, 0, \ldots, n.$$

Hence $\bar{\Phi}^{\text{up}}_i$, as well as Φ^{up}_j, can be computed by simply adapting the computational strategy developed for K^{up}. The approximations of R and L immediately follow by using (56).

5.4 Computation of the bound states and the norming constants

For the sake of completeness, we now give a brief description of the matrix-pencil method that we have recently developed for the identification of the bound states and the norming constants [6,8]. Setting $z_j = e^{i\lambda_j}$, the spectral function sum $S_\ell(\alpha)$ introduced in (9) can be represented as the monomial-power sum

$$S_\ell(\alpha) = \sum_{j=1}^{n} \sum_{s=0}^{m_j-1} c_{js}\alpha^s z_j^\alpha, \quad 0^0 \equiv 1,$$

where $c_{js} = (\Gamma_\ell)_{js}/s!$.

Letting $M = m_1 + \cdots + m_n$, the method allows one to compute the parameters $\{n, m_j, z_j\}$ and the coefficients $\{c_{js}\}$, given $S_\ell(\alpha)$ in $2N$ integer values ($N > M$)

$$\alpha = \alpha_0, \alpha_0 + 1, \ldots, \alpha_0 + 2N - 1, \quad \text{with} \quad \alpha_0 \in \mathbb{N}^+ = \{0, 1, 2, \ldots\},$$

under the assumption that a reasonable overestimate of M is known.

The basic idea of our method is the interpretation of $S_\ell(\alpha)$ as the general solution of a homogeneous linear difference equation of order M

$$\sum_{k=0}^{M} p_k S_{k+\alpha_0} = 0$$

whose characteristic polynomial (Prony's polynomial)

$$P(z) = \prod_{j=1}^{n}(z - z_j)^{m_j} = \sum_{k=0}^{M} p_k z^k, \quad p_M \equiv 1$$

is uniquely characterized by the z_j values we are looking for. The identification of the zeros $\{z_j\}$ allows one to compute the coefficients c_{js} by solving in the least squares sense a linear system.

For the computation of $\{z_j\}$ and then of the bound states λ_j, the given data are arranged in the two Hankel matrices of order N

$$(\mathbf{S}_\ell^0)_{ij} = S_\ell(i+j-2), \quad (\mathbf{S}_\ell^1)_{ij} = S_\ell(i+j-1), \qquad i,j = 1,2,\ldots,N.$$

To these matrices we then associate the $M \times M$ matrix-pencil

$$\mathbf{S}_{MM}(z) = (\mathbf{S}_{NM}^0)^*(\mathbf{S}_{NM}^1 - z\mathbf{S}_{NM}^0)$$

where the asterisk denotes the conjugate transpose. As proved in [8], the zeros z_j of the Prony polynomial, with their multiplicities, are exactly the generalized eigenvalues of the matrix-pencil $\mathbf{S}_{MM}(z)$. The simultaneous factorization of the matrices $\mathbf{S}_{NM}^0$ and $\mathbf{S}_{NM}^1$ by the generalized singular value decomposition allows us to compute the zeros z_j and then the bound states λ_j, as $\lambda_j = -i \log z_j$.

Analogous results can be obtained by a proper factorization of the augmented Hankel matrix $\mathbf{S}_\ell = [\mathbf{S}_{\ell,1}^0, \mathbf{S}_\ell^1]$, where $\mathbf{S}_{\ell,1}^0$ is the first column of $\mathbf{S}_{NM}^0$ and $\mathbf{S}_\ell^0$ is obtained by $\mathbf{S}_\ell^1$ by simply deleting its last column. As shown in [6], the QR factorization of $\mathbf{S}_\ell$ is as effective as its SVD factorization considered in [8], though its computational complexity is generally smaller.

The vector of coefficients

$$\mathbf{c} = [c_{1\,0}, \ldots, c_{1\,n_1-1}, \ldots, c_{L\,0}, \ldots, c_{L\,n_M-1}]^T$$

is then computed by solving (in the least square sense) the overdetermined linear system

$$\mathbf{K}_{NM}^0 \mathbf{c} = \mathbf{S}_\ell^0$$

where $\mathbf{S}_\ell{}^0 = [S_\ell(0),\ S_\ell(1), \ldots, S_\ell(N-1)]^T$ and $\mathbf{K}_{NM}^0$ is the Casorati matrix associated to the monomial powers $\{k^s z_j^k\}$ for $k = 1, \ldots, N-1$.

If $m_j \equiv 1$, the Casorati matrix $\mathbf{K}_{Nn}^0$ reduces to the Vandermonde matrix $(V)_{ij} = z_j^{i+1}$ of order $N \times n$ associated to the zeros $z_1, \ldots, z_n$. The solution of the Casorati system allows us to immediately compute the norming constants as $(\Gamma_\ell)_{js} = s! c_{js}$.

The coefficients $\{(\Gamma_r)_{js}\}$ are then obtained by solving, in the least square sense, a linear system whose vector of known data is given by $\Omega_r(\alpha) - \ell(\alpha)$ evaluated in a set of N equidistant points, with a sufficiently large $N > M$.

6 Examples

Let us now present two examples. The first one is a reflectionless case while the second one has reflection coefficients different from zero. Either example will be used in the next section to give numerical evidence of the effectiveness of our method.

Example 1 (One soliton potential)

Considering the initial potential for the NLS in the focusing case we take

$$u_0(x) = 2\mathbf{i}\eta e^{\mathbf{i}(2\xi x+\phi)}\mathrm{sech}(x_0 - 2\eta x) \tag{58}$$

where $\xi, \phi, x_0 \in \mathbb{R}$ and $0 \neq \eta \in \mathbb{R}$. As proved in [9], the corresponding initial value problem (1) can be solved exactly, as already considered in several papers and in particular in [5] and [4]. Let us note that $2\eta > 0$ represents the amplitude of the initial potential and $\mu_0 = x_0/2\eta$ is the initial peak position.

In this example the norming constants from the left and from the right are [4]:

$$\Gamma_\ell = 2\mathbf{i}\eta e^{x_0 - \mathbf{i}\phi} \quad \text{and} \quad \Gamma_r = -2i\eta e^{-x_0+\mathbf{i}\phi}. \tag{59}$$

Moreover, setting $a = \eta + \mathbf{i}\xi$, as it is immediate to check, the exact solution of the Volterra system (20) for $y \geq x$ is

$$\begin{pmatrix} K^{\text{up}}(x,y) \\ K^{\text{dn}}(x,y) \end{pmatrix} = -\frac{1}{1+e^{2(x_0-2\eta x)}} \begin{pmatrix} -\Gamma_\ell^* e^{-a^*(x+y)} \\ \dfrac{|\Gamma_\ell|^2}{2\eta} e^{-a^*(x+y)-2ax} \end{pmatrix},$$

while the exact solution of system (19) can be obtained by resorting to relation (27). Furthermore, the closed form solution of the Volterra system (22) is

$$\begin{pmatrix} M^{\text{up}}(x,y) \\ M^{\text{dn}}(x,y) \end{pmatrix} = -\frac{1}{1+e^{-2(x_0-2\eta x)}} \begin{pmatrix} \dfrac{|\Gamma_r|^2}{2\eta} e^{a^*(x+y)+2ax} \\ -\Gamma_r^* e^{a^*(x+y)} \end{pmatrix},$$

while the solution of system (21) can be deducted by using relation (27). As it represents a reflectionless case,

$$\rho(\alpha) = \ell(\alpha) = 0, \quad \alpha \in \mathbb{R},$$

so that the exact initial Marchenko kernels are [4]

$$\Omega_\ell(x) = \Gamma_\ell e^{-ax},$$
$$\Omega_r(x) = \Gamma_r e^{ax}.$$

Finally, the scattering matrix is

$$\mathbf{S}(\lambda) = \begin{pmatrix} T(\lambda) & L(\lambda) \\ R(\lambda) & T(\lambda) \end{pmatrix} = \begin{pmatrix} \dfrac{\lambda + ia^*}{\lambda - ia^*} & 0 \\ 0 & \dfrac{\lambda + ia^*}{\lambda - ia^*} \end{pmatrix}, \qquad \lambda \in \mathbb{C}^+.$$

Example 2 (Gaussian potential)

As a second example of the initial potential for the NLS, we take

$$u_0(x) = q_0 e^{\mathbf{i}\mu x} e^{-\frac{x^2}{\sigma}}, \tag{60}$$

where $q_0 > 0, \sigma > 0$ and $\mu \in \mathbb{R}$.

As in [11,18] we investigate the defocusing case in which the scattering coefficients $T(\lambda)$, $R(\lambda)$ and $L(\lambda)$ are all continuous functions and there are no bound states. Hence, in this case the following relations hold true

$$\Omega_\ell(\alpha) \equiv \rho(\alpha), \quad \Omega_r(\alpha) \equiv \ell(\alpha). \tag{61}$$

Moreover, we also consider the focusing case. In this case, whenever

$$q_0\sqrt{\pi\sigma} < \frac{\pi}{2},$$

there are no discrete eigenvalues. On the contrary, we have n discrete eigenvalues, all of them simple and having real part $-\frac{\mu}{2}$, if [10]

$$\left(n - \frac{1}{2}\right)\pi < q_0\sqrt{\pi\sigma} < \left(n + \frac{1}{2}\right)\pi. \tag{62}$$

As a result the spectral sums from the left and from the right (9) and (10) reduce to

$$S_\ell(\alpha) = \sum_{j=1}^{n} (\Gamma_\ell)_j e^{i\lambda_j\alpha} \quad \alpha > 0 \tag{63}$$

$$S_r(\alpha) = \sum_{j=1}^{n} (\Gamma_r)_j e^{i\lambda_j^*\alpha}, \quad \alpha < 0. \tag{64}$$

We also remark that the reflection coefficients $R(\lambda)$ and $L(\lambda)$ and the transmission coefficient $T(\lambda)$ are discontinuous at $\lambda = -\frac{\mu}{2}$ if [10]

$$q_0\sqrt{\pi\sigma} = \left(n - \frac{1}{2}\right)\pi$$

for some positive integer n.

7 Numerical results and conclusions

Test 1 (One soliton potential)

Let us consider as in [4] the initial potential (58) with $\xi = 1/10$, $x_0 = \phi = 0$ and $\eta = 2$. In order to compute the non-zero scattering parameters that in this case are the

norming constants, the bound states and the transmission coefficient, at first we solved the Volterra's system (20) and (22) with $L = 8$ and $n = 3000$ to obtain the following relative errors

$$\frac{\|K^{\text{up}} - \tilde{K}^{\text{up}}\|}{\|K^{\text{up}}\|} = 1.80e-06, \quad \frac{\|K^{\text{dn}} - \tilde{K}^{\text{dn}}\|}{\|K^{\text{dn}}\|} = 1.04e-07,$$
$$\frac{\|M^{\text{up}} - \tilde{M}^{\text{up}}\|}{\|M^{\text{up}}\|} = 1.07e-07, \quad \frac{\|M^{\text{dn}} - \tilde{M}^{\text{dn}}\|}{\|M^{\text{dn}}\|} = 1.80e-06,$$

where here and in the sequel quantities with $\sim$ denote the approximation of the exact function previously given and $\|\cdot\|$ denotes the maximum norm of the function involved in their computational areas. Identical relative errors are of course obtained for the remaining auxiliary functions, as a result of the symmetry properties (27) and (28).

Once these auxiliary functions are computed we numerically solved the equations for the Marchenko kernels from the right and from the left with the following relative errors:

$$\max_{x\in[0,L]} \frac{|\tilde{\Omega}_\ell(x) - \Omega_\ell(x)|}{|\Omega_\ell(x)|} \simeq \max_{x\in[-L,0]} \frac{|\tilde{\Omega}_r(x) - \Omega_r(x)|}{|\Omega_r(x)|} \simeq 3.24e-07,$$

where the symbol $\simeq$ means that the left term coincides with the right term up to the third decimal digit.

At this point, by using such kernels, we applied our matrix pencil method [6] to find a single bound state term, a norming constant from the left and a norming constant from the right with the following relative errors:

$$\frac{|\tilde{\lambda} - \lambda|}{|\lambda|} = 4.11e-09, \quad \frac{|\tilde{\Gamma}_\ell - \Gamma_\ell|}{|\Gamma_\ell|} \simeq \frac{|\tilde{\Gamma}_r - \Gamma_r|}{|\Gamma_r|} \simeq 3.24e-07.$$

Moreover, as a numerical check of our results, we verified the numerical validity of the algebraic property (8). The results are all satisfactory as Fig. 9 shows, where the behavior of the error function

$$E_s(\lambda) = \left\| \frac{1}{2}(\mathbf{S}^\dagger(\lambda)\mathbf{J}\mathbf{S}(\lambda) + \mathbf{S}(\lambda)\mathbf{J}\mathbf{S}^\dagger(\lambda)) - \mathbf{J} \right\|$$

is reported for $\lambda \in [-2L, 2L]$ in semilog scale.

Concerning the transmission coefficient, we can compute it by approximating at first the integral Φ^{up} defined in (36), and then using (52). In Table 1 we give the following relative errors we obtain for such a coefficient over segment of width $4L$ of three different lines

$$E_r(T) = \max_{\lambda\in[a,b]} \frac{|\tilde{T}(\lambda) - T(\lambda)|}{|T(\lambda)|}.$$

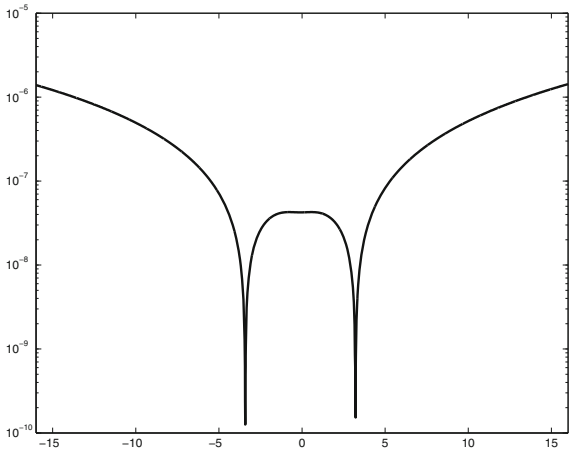

Fig. 9 $E_s(\lambda)$ in semi logarithmic scale

Table 1 $E_r(T)$ in the one soliton case

$[a, b]$	$E_r(T)$
$[-2L, 2L]$	$2.13e-07$
$[-2L+\mathbf{i}, 2L+\mathbf{i}]$	1.54e−07
$[-2L+5\mathbf{i}, 2L+5\mathbf{i}]$	1.74e−07

Test 2 (Gaussian potential)

Let us consider first the initial potential (60) in the defocusing case with $q_0 = 1.9$, $\mu = 1$, $\sigma = 2$ as in [11,18]. To this end, we computed the solution of systems (19)–(22) considering as in the soliton case $L = 8$ and $n = 3000$. Then we solved equations (29), (30), compute the scattering matrix and thus the Fourier transforms of the reflection coefficients. Our numerical method recognizes that, as theoretically expected, there are no bound states and relations (61) are numerically satisfied since we have the following errors:

$$\max_{x\in[0,2L]} |\Omega_\ell(x) - \rho(x)| = 1.08e-10, \quad \max_{x\in[-2L,0]} |\Omega_r(x) - \ell(x)| = 1.44e-09.$$

As in the one soliton case, we checked if our numerical results satisfy the algebraic property (8) for the scattering matrix, by considering in semi logarithmic scale the error function

$$E_{GD}(\lambda) = \left\| \frac{1}{2}(\mathbf{S}^\dagger(\lambda)\mathbf{S}(\lambda) + \mathbf{S}(\lambda)\mathbf{S}^\dagger(\lambda)) - \mathbf{I} \right\|$$

for $\lambda \in [-2L, 2L]$. As shown in Fig. 10 its numerical validity is satisfactory as in the soliton case.

Now let us investigate the focusing case considering the initial potential (60) with $q_0 = 2.5$, $\mu = 1$, $\sigma = 2$. As a result, inequality (62) implies that we have two simple bound states $\{\lambda_1, \lambda_2\}$ whose real part is $-1/2$. At first we computed the auxiliary

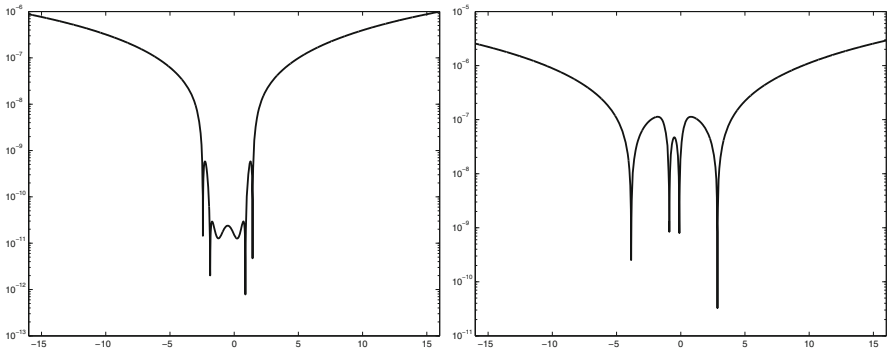

Fig. 10 E_{GD} (to the *left*) and E_{GF} (to the *right*) in semi logarithmic scale

functions by solving systems (19)–(22) with $L = 8$ and $n = 3000$, then we solved equations (29), (30), computed the scattering matrix and the Fourier transforms of the reflection coefficients. At this point, we applied the matrix pencil method described in Sect. 5.4 assuming that we have no more than five bound states. Our method recognizes that, as theoretically expected, we have two simple bound states having real part equal to $-\mu/2$. In fact, we get

$$\lambda_1 = -0.50 + 1.97\mathbf{i} \quad \lambda_2 = -0.50 + 0.79\mathbf{i}$$

with the corresponding norming constants

$$\begin{aligned} \Gamma_{\ell,1} &= 9.28 - 1.50\,10^{-8}\mathbf{i} \quad \Gamma_{\ell,2} = 3.74 - 1.76\,10^{-11}\mathbf{i} \\ \Gamma_{r,1} &= 9.28 + 1.50\,10^{-8}\mathbf{i} \quad \Gamma_{r,2} = 3.74 + 1.76\,10^{-11}\mathbf{i}. \end{aligned}$$

Finally, in Fig. 10 we represent in semi logarithmic scale the error function

$$E_{GF}(\lambda) = \left\| \frac{1}{2}(\mathbf{S}^{\dagger}(\lambda)\mathbf{J}\mathbf{S}(\lambda) + \mathbf{S}(\lambda)\mathbf{J}\mathbf{S}^{\dagger}(\lambda)) - \mathbf{J} \right\|$$

for $\lambda \in [-2L, 2L]$ that we have computed to check the validity of the algebraic property (7).

8 Conclusions

The numerical results show that our numerical method allows us to effectively compute all the scattering data in both the focusing and defocusing cases, provided the initial potential decays to zero at infinity and is at least continuous. This positive result is due to the possibility of knowing each pair of functions on the whole plane, by solving the corresponding Volterra system on a bounded computational triangle. The accuracy of the identification of the spectral parameters strongly depends on this result, since all the subsequent computations require the knowledge of the auxiliary functions on their

triangles. The computational complexity of our algorithm for evaluating the auxiliary functions is due to this consideration. As a consequence, it allows us to approximate them accurately in their unbounded supports and then to estimate at a high level of accuracy all the scattering data we are looking for.

We believe that the method can be extended, with the same accuracy of the results, in the presence of jump discontinuities of the initial potential. To this end, a numerically stable method for the solution of Fredholm integral equations (40), (41) and (43), (44) should be developed. The development of such a method should also be accompanied by an extensive numerical experimentation which requires the exact knowledge of scattering data in at least one case in which the initial potential has jump discontinuities. Considering that such research takes a rather long time, the development of such a method is postponed to a next paper.

Acknowledgments The research has been partially supported by INdAM (National Institute for Advanced Mathematics, Italy). The authors thank the referees for their suggestions and comments which allow us to improve the readability of the paper.

Appendix: Supports of the auxiliary functions

In this section we determine the supports of the auxiliary functions $K(x, y)$ and $M(x, y)$ if the potentials $u_0(x)$ and $v_0(x)$ have their supports in $[-L, L]$ whose identification, as explained before, is crucial for the computation of the auxiliary functions. It suffices to prove parts (2) of Lemmas 5.1 and 5.2 in [7], because the proofs of the other three parts of these two lemmas are immediate and proceed as in the discrete case.

Put

$$\nu(\bar{K}^{\,\mathrm{up}}; x) = \int_x^\infty |\bar{K}^{\,\mathrm{up}}(x, y)|\, dy, \qquad \nu(\bar{K}^{\,\mathrm{dn}}; x) = \int_x^\infty |\bar{K}^{\,\mathrm{dn}}(x, y)|\, dy;$$
$$Q(x) = \max(|u_0(x)|, |v_0(x)|), \qquad P(x) = \nu(\bar{K}^{\,\mathrm{up}}; x) + \nu(\bar{K}^{\,\mathrm{dn}}; x),$$

where Q and P are bounded [16]. Then for $x \le L$ and $x+y \ge 2L$ the integral equations (3.1) have zero right-hand sides, because $v_0(\frac{1}{2}(x+y)) = 0$ for $x+y > 2L$. Integrating the absolute values of $\bar{K}^{\,\mathrm{up}}(x, y)$ and $\bar{K}^{\,\mathrm{dn}}(x, y)$ with respect to $y \in (x, +\infty)$, we obtain

$$\nu(\bar{K}^{\,\mathrm{up}}; x) \le \int_x^L |u_0(z)| \nu(\bar{K}^{\,\mathrm{dn}}; z)\, dz,$$
$$\nu(\bar{K}^{\,\mathrm{dn}}; x) \le \int_x^L |v_0(z)| \nu(\bar{K}^{\,\mathrm{up}}; z)\, dz,$$

so that

$$0 \le P(x) \le \int_x^L Q(z) P(z)\, dz.$$

Hence iterating two times the last inequality we have

$$
\begin{aligned}
P(x) \le \int_x^L Q(z)P(z)\,dz &\le \int_x^L Q(z)\int_z^L Q(t)\int_t^L Q(w)P(w)\,dw\,dt\,dz \\
&\le \left(\int_x^L Q(w)P(w)\,dw\right)\left(\int_x^L Q(z)\int_z^L Q(t)\,dt\,dz\right) \\
&= \left(\int_x^L Q(w)P(w)\,dw\right)\left(\int_x^L -\frac{1}{2}\frac{d}{dz}\left(\int_z^L Q(t)\,dt\right)^2 dz\right) \\
&= \left(\int_x^L Q(w)P(w)\,dw\right)\left[-\frac{1}{2}\left(\int_z^L Q(t)\,dt\right)^2\right]_{z=x}^{z=L} \\
&= \left(\int_x^L Q(w)P(w)\,dw\right)\frac{1}{2}\left(\int_x^L Q(t)\,dt\right)^2.
\end{aligned}
$$

Thus iterating $n-1$ times we get

$$
0 \le P(x) \le \frac{1}{n!}\left[\int_x^L Q(w)\,dw\right]^n \int_x^L Q(z)P(z)\,dz.
$$

Taking the limit as $n \to +\infty$, we get $P(x) = 0$ and hence $\bar{K}^{\,\mathrm{up}}(x, y) = \bar{K}^{\,\mathrm{dn}}(x, y) = 0$ for almost every $y > x$, as claimed. The proof of part (2) of Lemma 5.2 is analogous.

References

1. Ablowitz, M.: Nonlinear dispersive waves. Cambridge Univ. Press, Cambridge (2011)
2. Ablowitz, M.J., Clarkson, P.A.: Solitons, nonlinear evolution equations and inverse scattering. Cambridge University Press, Cambridge (1991)
3. Ablowitz, M.J., Prinari, B., Trubatch, A.D.: Discrete and continuous nonlinear Schrödinger systems. Cambridge University Press, Cambridge (2004)
4. Aricò, A., Rodriguez, G., Seatzu, S.: Numerical solution of the nonlinear Schrödinger equation, starting from the scattering data. Calcolo **48**(1), 75–88 (2011)
5. Aricò, A., van der Mee, C., Seatzu, S.: Structured matrix numerical solution of the nonlinear Schrödinger equation by the inverse scattering transform. Electron. J. Differ. Equ. **15**, 1–21 (2009)
6. Fermo, L., van der Mee, C., Seatzu, S.: Parameter estimation of monomial-exponential sums in one and two variables. Appl. Math. Comput. **258**, 576–586 (2015)
7. Fermo, L., van der Mee, C., Seatzu, S.: Emerging problems in approximation theory for the numerical solution of the nonlinear Schrödinger equation. Publication de l'Institut Mathématique **96**, 125–141 (2014)
8. Fermo, L., van der Mee, C., Seatzu, S.: Parameter estimation of monomial-exponential sums. Electron. Trans. Numer. Anal. **41**, 249–261 (2014)
9. Hasegawa, A., Tappert, F.: Transmission of stationary nonlinear optical pulses in dispersive dielectric fibers. I. Anomalous dispersion. Appl. Phys. Lett. **23**(3), 142–144 (1973)
10. Klaus, M., Shaw, J.K.: On the eigenvalues of Zakharov-Shabat systems. SIAM J. Math. Anal. **34**, 759–773 (2003)
11. Osborne, A.R.: Numerical inverse scattering transform for the periodic, defocusing nonlinear Schrödinger equation. Phys. Lett. A **176**, 75–84 (1993)
12. Shaw, J.K.: Mathematical principles of optical fiber communications. In: CBMS-NSF Regional Conference Series in Applied Mathematics, vol. 76 (2004)
13. Stoer, J., Bulirsch, R.: Introduction to numerical analysis. Springer Verlag, New York (1980)

14. Trogdon, T., Olver, S.: Numerical inverse scattering for the focusing and defocusing nonlinear Schrödinger equations. Proc. R. Soc. A **469**, 20120330 (2013)
15. Trogdon, T., Olver, S.: Riemann-Hilbert problems, their numerical solution, and the computation of nonlinear special functions. SIAM, Philadelphia (2015, in press)
16. van der Mee, C.: Nonlinear evolution models of integrable type. SIMAI e-Lecture Notes, vol. 11, Torino (2013)
17. Zakharov, V.E., Shabat, A.B.: Exact theory of two-dimensional self-focusing and one dimensional self-modulation of waves in nonlinear media. Sov. Phys. JETP **34**, 62–69 (1972)
18. Wahls, S., Vincent Poor, H.: Fast numerical nonlinear Fourier transforms. arXiv:1402.1605v2 (submitted)